through 360° did not reveal a single conformation that explains all of the observed data. Thus, both ends of the oligonucleotide are flexible and exist in a mixture of conformers.

Three additional qualitative models, models II–IV, were also constructed and examined. The values of the torsion angles used to construct the various structures are listed in Table SIV (supplementary material). For example, model III made use of the A- and B-DNA torsion angles reported by Lippard (Figure S5, supplementary material).[23] No noteworthy differences were observed for models II–IV compared to model I. Thus, our conclusions based on our initial qualitative model I appear reasonable.

In summary, the use of ^{13}C NMR spectroscopy to study drug–oligonucleotide adducts holds considerable promise. The method clearly pinpoints sugar conformational changes. A predominantly S $\rightarrow$ predominantly N conformational change shifts the ^{13}C signal of C3′ into a spectral region of the 2D HMQC spectrum that otherwise lacks signals except for the 3′-terminal C3′ signal. Thus, it is possible that such a conformational change can be observed in relatively large oligonucleotides where ^{1}H signal overlap would prevent assessment of ^{1}H–^{1}H coupling constants, which otherwise are useful for assigning sugar pucker. Furthermore, as in the case of cross-linked adducts studied here, the ^{1}H–^{1}H coupling pattern may not be resolved, precluding the use of this method for assigning sugar pucker. Clearly, the ^{1}H and ^{13}C methods are complementary and both can be very useful. Finally, ^{13}C signals are useful in defining metal-binding sites. The same advantages of this method for mononucleotide studies are passed on to oligonucleotide studies.[25] Signals for carbons remote from the metal binding site appear to be most useful.

Acknowledgment. We thank the National Institutes of Health for support (GM 29222 to L.G.M.), as well as for partial support for the instrument purchase, which was also supported in part by the National Science Foundation. We acknowledge several helpful discussions with Prof. David Live.

Registry No. d(TGGT), 87471-59-8; Pt(en)Cl$_2$, 14096-51-6; d(TGGT)-Pt(en), 132260-29-8.

Supplementary Material Available: Tables of the ^{1}H and ^{13}C chemical shifts and the ^{13}C–^{1}H coupling constants of d(TGGT)-Pt(en) at 40 °C and of the torsional angles used for models I–IV and figures of the full HMBC spectrum of d(TGGT) at 12 °C, the sugar region of the HOHAHA spectrum of d(TGGT) at 40 °C, the full NOESY spectrum of d(TGGT)-Pt(en) at 12 °C, and structural models I and III (10 pages). Ordering information is available on any current masthead page.

η^2-Dihydrogen on the Brink of Homolytic Cleavage: *trans*-[Os(H···H)H(PEt$_2$CH$_2$CH$_2$PEt$_2$)$_2$]$^+$ Has Spectroscopic and Chemical Properties between Those of the Isoelectronic Complexes *trans*-[OsH(PPh$_2$CH$_2$CH$_2$PPh$_2$)$_2$(η^2-H$_2$)]$^+$ and ReH$_3$(PPh$_2$CH$_2$CH$_2$PPh$_2$)$_2$

Kelly A. Earl, Guochen Jia, Patricia A. Maltby, and Robert H. Morris*

Contribution from the Department of Chemistry and the Scarborough Campus, University of Toronto, Toronto, Ontario M5S 1A1, Canada. *Received September 5, 1990*

Abstract: The new, octahedral complex *trans*-[OsH(dppe)$_2$(η^2-H$_2$)]$^+$, **1Os**, dppe = PPh$_2$CH$_2$CH$_2$PPh$_2$, prepared by addition of H$^+$ to *cis*-OsH$_2$(dppe)$_2$, has a rapidly spinning dihydrogen ligand with an unusually long (0.99 Å) H–H distance according to the T_1 NMR method. Additional evidence for this is a short T_1 value for the H$_2$ ligand in the complex *trans*-[OsH(dppe-d_{20})$_2$(η^2-H$_2$)]$^+$ and a large ^1J(H,D) value (25.5 Hz) for *trans*-[OsH(dppe)$_2$(η^2-HD)]$^+$, **1Os**-d_1. The known complex *trans*-[Os(H···H)H(depe)$_2$]$^+$, **2Os**, depe = PEt$_2$CH$_2$CH$_2$PEt$_2$, has properties (δH, J(H,D), T_1^{-1}) between those of **1Os** and ReH$_3$(dppe)$_2$, **3Re**, a true pentagonal, bipyramidal trihydride with r(H···H) $\sim$ 2 Å; e.g., the J(H···D) coupling for *trans*-[Os(H···D)D(depe)$_2$]$^+$, **2Os**-d_2, is the unusual value of $\sim$11.5 Hz, whereas for **3Re**-d_2 it is 0 Hz, as expected. Significantly the 11.5-Hz value varies by ±1 Hz depending on the solvent and temperature. VT NMR spectra of **2Os**-d_2 conclusively show that J(H···D) is not lost but is averaged by intramolecular H/D atom exchange; at 325 K, J_{av}(H,D) = 3.8 Hz. There are three possible answers to the question as to whether there is homolytic cleavage of H$_2$ in **2Os**: (1) no H–H cleavage so that **2Os**, like **1Os**, has a stretched, rapidly spinning dihydrogen ligand with r(H–H) = 1.2 Å; (2) complete H–H bond breaking to give an unusual trihydride with two closely spaced hydrides, 1.4–1.5 Å apart; and (3) a rapidly equilibrating mixture ($\Delta G^{\ddagger} \le 9$ kcal mol^{-1}) of Os(H)(η^2-H$_2$) and Os(H)$_3$ tautomers. The rapid equilibrium model (3) with the Os(H)$_3$ tautomer in greater abundance fits all available data for **2Os** and other complexes of Os with small J(H···D) couplings. The equilibrium shifts toward the dihydrogen form with an increase in temperature or on going from acetone-d_6 to CD$_2$Cl$_2$ as signaled by changes in δ(H$_2$), T_1(H$_2$), and J(H,D) values. An alternative answer (2) cannot be ruled out since closely spaced hydrides might move closer together with these changes in conditions and produce the same spectral changes. Also included are X-ray diffraction structural data for the three complexes, their infrared, chemical, and electrochemical properties as well as differences in NMR properties: rates of intramolecular H-atom exchange, chemical shifts, and coupling constants of the isotopomers **1Os**-d_1, **2Os**-d_1, **2Os**-d_2, and **3Re**-d_2. **1Os** retains the H–H bond because it has lower energy 5d electrons than **2Os** or **3Re**, and the dppe ligands are small enough to allow an undistorted octahedral coordination geometry. **3Re** gives shorter T_1 times for hydride and phosphorus nuclei than expected solely from dipolar relaxation by neighboring protons.

Several η^2-dihydrogen complexes have characteristics indicative of a short (<1 Å) H–H distance and a relatively weak interaction with the metal.[1-8] The large dipolar coupling between the η^2-H$_2$ nuclei can be observed by NMR in the solid state,[9] and this

0002-7863/91/1513-3027$02.50/0 © 1991 American Chemical Society

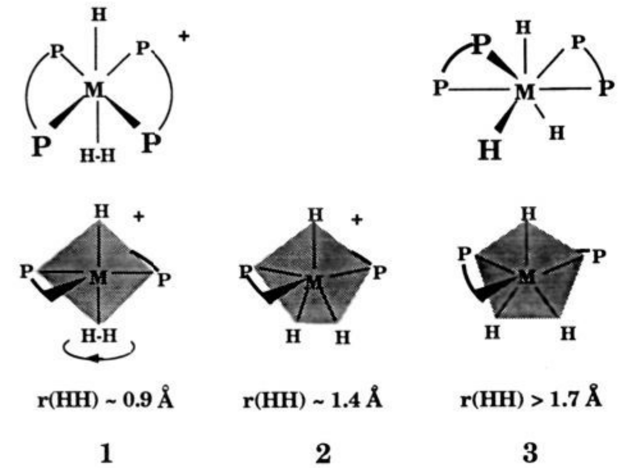

Figure 1. (1) Two views of an octahedral complex $[MHL_2(\eta^2\text{-}H_2)]^+$ with a spinning η^2-H_2 ligand. (2) A distorted pentagonal-bipyramidal (almost octahedral) complex with separate, closely spaced hydride ligands. (3) Two views of a pentagonal-bipyramidal geometry for a trihydride like ReH_3L_2 (**3Re**). Only the phosphorus atoms of the ditertiaryphosphine (L) which are coplanar with the hydrogen ligands are shown in the bottom view.

coupling results in short T_1 times for the dihydrogen nuclei in solution. NMR also provides evidence that the dihydrogen ligand is spinning rapidly or quantum mechanically tunnelling in the plane perpendicular to the metal–dihydrogen direction (e.g., Figure 1, structure **1**).[1,9] The ^1J(H,D) couplings of corresponding η^2-*HD* complexes are usually 30 ± 4 Hz, somewhat reduced from 43 Hz for HD(g). Usually couplings $^2J(H_2,P)$ to phosphine ligands in the complexes are characteristically small (<5 Hz) compared to couplings between hydride ligands and phosphorus donor nuclei.

An important current problem is the elucidation of the structures of complexes having properties between the ones mentioned above for H_2 complexes (H–H distance less than 1 Å) and those of dihydrides with usual H···H distances of greater than 1.6 Å. For example, several complexes which have *J*(H,D) coupling constants that fall between 25 and 12 Hz have been recently reported.[10-15] Usually these complexes are more hydride-like: the H_2 is not displaced easily and $^2J(H,P) > 4$ Hz.[16] How should the structure and bonding of these "intermediate dihydrides" be viewed? These questions are particularly difficult to answer for polyhydride complexes because their NMR properties are averaged by fluxional processes. The shortest distance reported so far for separate hydrides in a polyhydride complex is *r*(H···H) = 1.6 Å (by neutron diffraction) in $OsH_6(PiPr_3)_2$.[17] A recent example of a complex with an "intermediate" H···H distance of 1.08 Å (X-ray) is $[ReH_4(cyttp)(H\cdots H)]^+$.[18]

Another ambiguous complex is *trans*-$[Os(H\cdots H)H(depe)_2]^+$, **2Os**, depe = $PEt_2CH_2CH_2PEt_2$.[1,19,20] The T_1 NMR method, when applied to solutions of **2Os**, gives an H···H distance of 1.1 Å if the H_2 ligand is spinning and has a shorter correlation time than other protons in the molecule (structure **1**).[1] Alternatively the H···H distance could be 1.4 Å if the closely spaced hydrides do not have rapid rotational motion (**2**). In this case quantum mechanical exchange coupling is possible as demonstrated for the complexes $[Ir(C_5H_5)(H)_3(L)]^+$.[21,22] A third possibility is that there is a rapid equilibrium between a spinning dihydrogen tautomer, **1**, and a dihydride tautomer, **2** or **3**, to produce averaged properties. There are a few examples of slower equilibria of this type where resonances due to the two tautomers can be resolved in the slow-exchange spectra at low temperature: for $[ReH_4(CO)(PMe_2Ph)_3]^+$,[23] $WH_2(CO)_3(PR_3)_2$,[24] $[RuCpH_2(dmpe)]^+$,[12] and $[RuH_2(O_2CCF_3)_2(PR_3)_2]^+$.[25] Here we weigh the evidence for the various possible structures for **2Os** and make comparisons to closely related complexes: the new η^2-H_2 complex *trans*-$[OsH(dppe)_2(\eta^2\text{-}H_2)]^+$, **1Os**, dppe = $PPh_2CH_2CH_2PPh_2$, with octahedral structure **1** and the known trihydride, $ReH_3(dppe)_2$, **3Re**,[26,27] with pentagonal-bipyramidal structure **3**. The well-characterized complexes $[M(H)(ditertiaryphosphine)_2(H_2)]^+$, M = Fe, Ru,[1,28-31] and $[M(H)(tetraphosphine)(H_2)]^+$, M = Fe, Os,[32] also provide useful contrasts to **2Os**. Thus throughout this paper the formula *trans*-$[Os(H\cdots H)(H)L_2]^+$ is used to emphasize the schizophrenic nature of **2Os**.

Results

Preparation of the Dihydrogen Complexes. The dppe complex, **1Os**, is readily prepared in high yields as the BF_4^- salt by reaction of a suspension of $Os(H)_2(dppe)_2$ (90% cis, 10% trans) in ether or THF with ≥1 equiv of $HBF_4{\cdot}Et_2O$ under H_2, Ar, or N_2 (eq 1). Pale white **1Os** precipitates immediately. The starting

$$OsH_2(dppe)_2 + HBF_4 \rightarrow \underset{\mathbf{1Os}}{trans\text{-}[Os(H)(dppe)_2(\eta^2\text{-}H_2)]BF_4} \qquad (1)$$

complex, $OsH_2(dppe)_2$, can be prepared from *cis*-$OsCl_2(dppe)_2$ by sequential reactions with $LiAlH_4$ and then $NaBH_4$[33] or, more conveniently, by reaction with H_2 (1 atm) as in eq 2. This reaction is promoted by $NaBPh_4$ (a source of active Na^+) and actually

---

(1) Bautista, M. T.; Earl, K. A.; Maltby, P. A.; Morris, R. H.; Schweitzer, C. T.; Sella, A. *J. Am. Chem. Soc.* **1988**, *110*, 7031–7036.

(2) Bianchini, C.; Mealli, C.; Meli, A.; Peruzzini, M.; Zanobini, F. *J. Am. Chem. Soc.* **1988**, *110*, 8725–8726.

(3) Crabtree, R. H.; Hamilton, D. G. *Adv. Organomet. Chem.* **1988**, *28*, 299–338.

(4) Hamilton, D. G.; Crabtree, R. H. *J. Am. Chem. Soc.* **1988**, *110*, 4126–4133.

(5) Hampton, C.; Cullen, W. R.; James, B. R. *J. Am. Chem. Soc.* **1988**, *110*, 6918–6919.

(6) Kubas, G. J. *Acc. Chem. Res.* **1988**, *21*, 120.

(7) Morris, R. H.; Sawyer, J. F.; Shiralian, M.; Zubkowski, J. *J. Am. Chem. Soc.* **1985**, *107*, 5581–5582.

(8) Van Der Sluys, L. S.; Eckert, J.; Eisenstein, O.; Hall, J. H.; Huffman, J. C.; Jackson, S. A.; Koetzle, T. F.; Kubas, G. J.; Vergamini, P. J.; Caulton, K. G. *J. Am. Chem. Soc.* **1990**, *112*, 4831–4841.

(9) Zilm, K. W.; Merrill, R. A.; Kummer, M. W.; Kubas, G. J.; *J. Am. Chem. Soc.* **1986**, *108*, 7837–7839.

(10) Bautista, M. T.; Earl, K. A.; Morris, R. H. *Inorg. Chem.* **1988**, *27*, 1124–1126.

(11) Bianchini, C.; Mealli, C.; Peruzzini, M.; Zanobini, F. *J. Am. Chem. Soc.* **1987**, *109*, 5548–5549.

(12) Chinn, M. S.; Heinekey, D. M. *J. Am. Chem. Soc.* **1987**, *109*, 5865–5867.

(13) Harman, W. D.; Taube, H. *J. Am. Chem. Soc.* **1990**, *112*, 2261–2263.

(14) Siedle, A. R.; Newmark, R. A.; Korba, G. A.; Pignolet, L. H.; Boyle, P. D. *Inorg. Chem.* **1988**, *27*, 1593–1598.

(15) Collman, J. P.; Wagenknecht, P. S.; Hembre, R. T.; Lewis, N. S. *J. Am. Chem. Soc.* **1990**, *112*, 1294–1295.

(16) Cotton, F. A.; Luck, R. L. *J. Chem. Soc., Chem. Commun.* **1988**, 1277–1278.

(17) Howard, J. A. K.; Johnson, O.; Koetzle, T. F.; Spencer, J. L. *Inorg. Chem.* **1987**, *26*, 2930–2933.

(18) Kim, Y.; Deng, H.; Meek, D. W.; Wojcicki, A. *J. Am. Chem. Soc.* **1990**, *112*, 2798–2800.

(19) Earl, K. A.; Morris, R. H.; Sawyer, J. F. *Acta Crystallogr., Sect. C* **1989**, *C45*, 1137–1139.

(20) Bautista, M.; Earl, K. A.; Morris, R. H.; Sella, A. *J. Am. Chem. Soc.* **1987**, *109*, 3780–2.

(21) Zilm, K. W.; Heinekey, D. M.; Millar, J. M.; Payne, N. G.; Neshyba, S. P.; Duchamp, J. C.; Szczyrba, J. *J. Am. Chem. Soc.* **1990**, *112*, 920–929.

(22) Heinekey, D. M.; Millar, J. M.; Koetzle, T. F.; Payne, N. G.; Zilm, K. W. *J. Am. Chem. Soc.* **1990**, *112*, 909–919.

(23) Luo, X.; Crabtree, R. H. *J. Chem. Soc., Chem. Commun.* **1990**, 189–190.

(24) Khalsa, G. R. K.; Kubas, G. J.; Unkefer, C. J.; van Der Sluys, L. S.; Kubat-Martin, K. A. *J. Am. Chem. Soc.* **1990**, *112*, 3855–3860.

(25) Arliguie, T.; Chaudret, B. *J. Chem. Soc., Chem. Commun.* **1989**, 155–157.

(26) Ginsberg, A. P.; Tully, M. E. *J. Am. Chem. Soc.* **1973**, *95*, 4749–4751.

(27) Bau, R.; Carroll, W. E.; Hart, D. W.; Teller, R. G. *Adv. Chem. Ser.* **1978**, *167*, 73–92.

(28) Cappellani, E. P.; Maltby, P. A.; Morris, R. H.; Schweitzer, C. T.; Steele, M. R. *Inorg. Chem.* **1989**, *28*, 4437–4438, and references therein.

(29) Ricci, J. S.; Koetzle, T. F.; Bautista, M. T.; Hofstede, T. M.; Morris, R. H.; Sawyer, J. F. *J. Am. Chem. Soc.* **1989**, *111*, 8823–8827.

(30) Eckert, J.; Blank, H.; Bautista, M. T.; Morris, R. H. *Inorg. Chem.* **1989**, *29*, 747–750.

(31) Bautista, M. T.; Cappellani, E. P.; Drouin, S. D.; Morris, R. H.; Schweitzer, C. T.; Sella, A.; Zubkowski, J. *J. Am. Chem. Soc.*, in press.

(32) Bautista, M. T.; Earl, K. A.; Maltby, P. A.; Morris, R. H. *J. Am. Chem. Soc.* **1988**, *110*, 4056–7.

(33) Maltby, P. A. MSc Thesis, University of Toronto, 1988.

proceeds via two successive intermediates, $[Os(Cl)(dppe)_2(H_2)]^+$ and **1Os**.[28]

$$OsCl_2(dppe)_2 + 2Na^tBuO + 2H_2 \rightarrow OsH_2(dppe)_2 + 2NaCl + 2^tBuOH \quad (2)$$

The route to **2Os** is eq 3, the details of which were reported in a brief form previously.[20] This procedure was based on the preparation of the analogous dinitrogen complexes *trans*-$[M(H)(depe)_2(N_2)]BPh_4$.[34]

$$trans\text{-}Os(Cl)(H)(depe)_2 + NaBPh_4 + H_2 \rightarrow trans\text{-}[Os(H\cdots H)(H)(depe)_2]BPh_4 + NaCl \quad (3)$$

Complexes **1Os** and **2Os** are soluble and stable to loss of H_2 in THF, acetone, or CH_2Cl_2 (for at least 30 min) under Ar at 22°; **1Os** has a low solubility in THF. Dihydrogen is slowly replaced by 1 atm of CO in acetone solution to give the corresponding carbonyl complexes *trans*-$[Os(H)(CO)L_2]^+$ with the relative rates of reactions increasing as **2Os** ≪ **1Os**; the half-lives of **2Os** and **1Os** at 20° are 170 and <10 h, respectively. The half-life for D_2 addition to **2Os** is 180 h.[20] Thus **2Os** has more trihydride character than **1Os** assuming that loss of H_2 is rate-determining in these substitution reactions.

Structural Information from Diffraction Studies. The X-ray diffraction study of the BF_4^- salt of **1Os** revealed that the OsP_4 structural unit is perfectly square-planar (*trans*-P–Os–P angle of 176°; cf. Figure 1, **1**) and consistent with an octahedral *trans*-$[Os(H)(dppe)_2(\eta^2\text{-}H_2)]^+$ formulation.[35] The osmium-bonded hydrogens were not located accurately. However the H–H distance of 0.99 Å determined by NMR methods (see below) is easily accommodated by the large Os ion without close contacts to neighboring atoms; the analogous complex with the smaller Fe(II) ion has a proportionally shorter H–H distance of 0.82 (1) Å (neutron diffraction).[29] The corresponding P–Re–P angles in the pentagon defined by three H and two P of the pentagonal-bipyramidal complexes **3Re** and $Re(H)_3(PMePh_2)_4$ are 151.5 (5)°[27] and 136.1 (1)°,[36] respectively (Figure 1, **3**). Figure 1 emphasizes the close relationship between the equatorial plane of octahedral *trans*-$[M(H)(dppe)_2(H_2)]^+$ M = Fe, Os (**1**), and that of the pentagonal plane of the Re complexes, a relationship which might suggest a low energy of interconversion of the $M(H)(\eta^2\text{-}H_2)$ and $M(H)_3$ forms (see below).

Crystals of **2Os** have also been examined by X-ray diffraction, but disorder of the depe ligands prevented location of H atoms.[19] No distinction could be made between a distorted octahedral geometry expected for *trans*-$[Os(H)L_2(\eta^2\text{-}H_2)]^+$ versus a pentagonal-bipyramidal geometry expected for $[Os(H)_2(H)L_2]^+$ because of the disordered positions of the phosphorus atoms. In fact a mixture of tautomers **1** and **2** might account for the disorder; from this structure determination the most likely P–Os–P angles for the trihydride tautomer is 150° (for P–Os–P in the pentagonal plane of the PBP) and for the dihydrogen form is 164° (P–Os–P angle of distorted octahedron). A disordered structure with closely spaced hydrides (Figure 1, **2**) could also fit the data.

Spectroscopic Properties. Vibrational spectroscopy reveals the presence of a terminal hydride stretching mode, ν(M–H), for the complexes but not the weak ν(H–H) absorption.[6] The ν(M–H) mode for **1Os** correctly fits the periodic trend of increasing frequency going from Fe to Ru to Os in the isostructural complexes *trans*-$[M(H)(dppe)_2(\eta^2\text{-}H_2)]^+$ (Table I). Typically the frequency for isostructural complexes increases as the metal changes down the group.[37,38] The neutral trihydride, $Re(H)_3(dppe)_2$, has a strong mode, ν(Re–H), at a lower frequency (1860 cm^{-1}) than these cationic complexes. The two-band pattern for **2Os** as the BPh_4^- salt in Nujol (1983, 1937 cm^{-1}, Table I) might be due to a pentagonal-bipyramidal trihydride form like **3Re** or more likely to a mixture of an octahedral $(H)(\eta^2\text{-}H_2)$ complex (**1**, Figure 1) and a trihydride complex with structure **2** or **3**; this could explain the disorder of the X-ray structure. The BF_4^- salt of **2Os** appears to be exclusively in the trihydride form in the solid state with a single band at 1924 cm^{-1} (Table I). **2Os** gives only one peak in solution, and the frequency is about 55 cm^{-1} lower than that predicted (1990 cm^{-1}) based on the periodic trend in ν(M–H) of isostructural complexes *trans*-$[M(H)(depe)_2(\eta^2\text{-}H_2)]^+$, M = Fe, Ru (Table I). This unexpectedly low frequency suggests that **2Os** is in predominantly the trihydride form (**2** or **3**) in solution considering that **3Re** also has a low stretching frequency, ν(Re–H).

Table I. Hydride Stretching Frequencies of the Complexes **1Os**, **2Os**, and **3Re** and Related Complexes

	complex	ν(M–H), cm^{-1} Nujol	ν(M–H), cm^{-1} CH_2Cl_2
	$[Fe(H)(dppe)_2(H_2)]BF_4$	1919[7]	
	$[Ru(H)(dppe)_2(H_2)]BF_4$	1961[7]	
1Os	$[Os(H)(dppe)_2(H_2)]BF_4$	1997	2020
	$[Fe(H)(depe)_2(H_2)]BPh_4$	1887[31]	
	$[Ru(H)(depe)_2(H_2)]BPh_4$	1964[31]	
2Os	$[Os(H\cdots H)(H)(depe)_2]BPh_4$	1983, 1937	1939
	$[Os(H\cdots H)(H)(depe)_2]BF_4$	1924	1939
3Re	$Re(H)_3(dppe)_2$	1860	

Table II. ^1H NMR Data at 200 MHz in the Hydride Region for the Complexes

complex	*T*, K	δ(M–H)	^2J(H, P)	$\delta(H_2)$	$^2J(H_2, P)$
1Os	294	−7.35	nr[a]	−7.35	nr[a]
CD_2Cl_2	210	−9.0[b]	−17	−6.8[c]	−5 ± 2
2Os	291	−9.73	−9.5	−9.73	−9.5
acetone-d_6	200	−9.68	−17.5	−10.03[d]	−5.5
2Os	296	−9.75	−9.5	−9.75	−9.5
CD_2Cl_2	202	−9.83	−17.8	−9.88[e]	−5
3Re	290	−8.0	−17	−8.0	−17
CD_2Cl_2	210	−7.6	−21	−8.2[f]	−14

[a] Not resolved, broad singlet. [b] Temperature dependent: $\delta(M\text{–}H) = 0.0056T - 10.20$. [c] Temperature dependent: $\delta(H_2) = -0.0014T - 6.49$. [d] Broad, temperature dependent: $\delta(H_2) = 0.0029T - 10.61$. [e] Broad, temperature dependent: $\delta(H_2) = 0.00118T - 10.21$. [f] Two separate, equivalent hydrides: $^2J(H_2, H) = 10$ Hz.

Low-Temperature ^1H NMR Spectra in the Hydride Region. The temperature-dependent ^1H NMR spectra of the complexes in the hydride region give the most structural and dynamic information about the dihydrogen ligands in complexes in solution.[1] The 200-MHz spectra for complexes **1Os** and **2Os** are shown in Figures 2 and 3. Figure 2 allows a comparison of the spectra of **3Re** with those of **1Os**.

At 210 K, 200 MHz, the resonance of the terminal hydride (trans to the H···H unit) of **1Os** and **2Os** is a well-resolved, binomial quintet with the magnitude of the ^2J(H,P) constants typical of couplings between cis ^1H and ^{31}P nuclei in bonds at 90° angles (see Table II). For example, the carbonyl complexes *trans*-$[Os(H)(CO)L_2]^+$ have ^2J(H,P) of −19.2 Hz for L = dppe and −20.4 Hz for L = depe. Recent work verifies the negative sign of this coupling constant.[39,40] There is no resolved coupling pattern on this quintet [$^2J(H,H_2) < 1$ Hz] for **1Os** although the peaks for **2Os** are broad enough to contain a coupling of up to 3 Hz. By contrast the separate hydride between the phosphorus atoms in **3Re** (Figure 1) gives a triplet of quintets with $|^2J(H,(H)_2)| = 10$ Hz and $|^2J(H,P)| = 21$ Hz at 213 K (Figure 2[26]). At 290 K three equivalent hydrides in **3Re** give a quintet with $|^2J(H,P)| = 17.5$ Hz, close to the predicted average ($0.333 \times 21 + 0.666 \times 14 = 16.3$) where 21 and 14 Hz are the ^2J(H,P) values observed at low temperature (Table II). The magnitude of the ^2J(H,P) coupling is not diagnostic of pentagonal-bipyramidal coordination

---

[34] Bancroft, G. M.; Mays, M. J.; Prater, B.; Stefanini, F. P. *J. Chem. Soc. A* **1970**, 2146–2149.

[35] Farrar, D. H.; Maltby, P. A.; Morris, R. H. *Acta Crystallogr., Sect. C*, in press.

[36] Cotton, F. A.; Luck, R. L. *Inorg. Chem.* **1989**, *28*, 2181–2186.

[37] Hlatky, G. G.; Crabtree, R. H. *Coord. Chem. Rev.* **1985**, *65*, 1–48.

[38] Morris, R. H.; Nassif, O. Unpublished review of metal hydride vibrations.

[39] Benn, R.; Joussen, E.; Lehmkuhl, H.; Lôpez Ortiz, F.; Rufinska, A. *J. Am. Chem. Soc.* **1989**, *111*, 8754–8756.

[40] Eisenschmid, T. C.; McDonald, J.; Eisenberg, R.; Lawler, R. G. *J. Am. Chem. Soc.* **1989**, *111*, 7267–7269, and references therein.

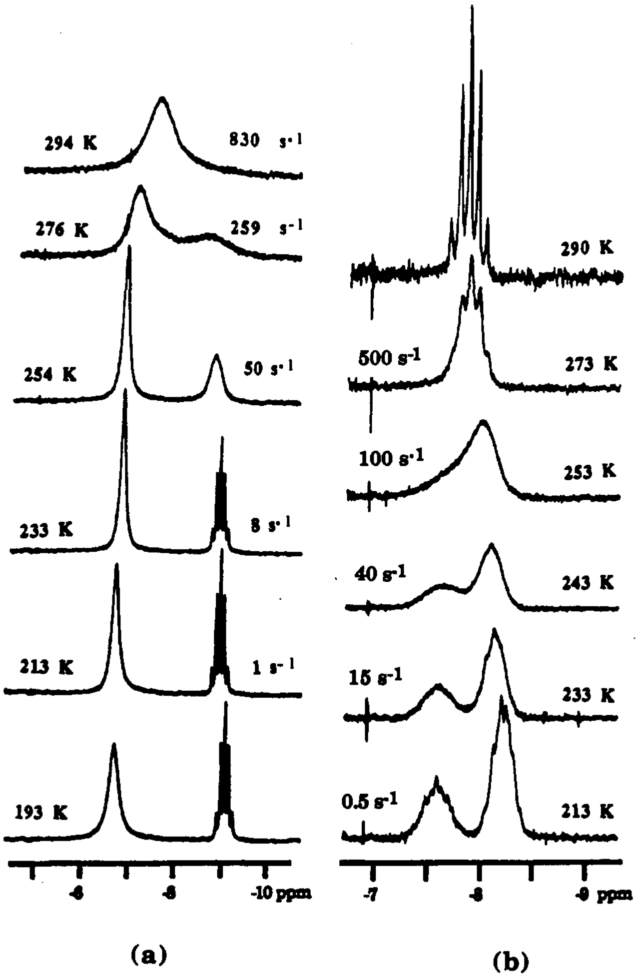

Figure 2. The variable-temperature 200-MHz ^1H NMR spectra in the high field region of isoelectronic (a) $[Os(H)(dppe)_2(H_2)]BF_4$, **1Os**, in CD_2Cl_2 and (b) $Re(H)_3(dppe)_2$, **3Re**, in CD_2Cl_2. Temperatures and rate constants for the intramolecular H-atom site-exchange process are also provided.

since the octahedral complex $ReH(CO)(dppe)_2$ gives the same value of 21 Hz.[41]

The broad dihydrogen resonance at 210 K is found downfield of the quintet for **1Os** (Figure 2) as in related Fe and Ru complexes $[MH(dppe)_2(H_2)]^+$. By contrast it is slightly upfield for **2Os** in acetone-d_6 (Figure 3) and superimposed on this quintet in CD_2Cl_2 (Table II). The two equivalent hydrides in **3Re** are also upfield. The temperature dependence of $\delta(H_2)$ of **2Os** is evidence for a rapid equilibrium, even at 210 K, between a dihydrogen form of **2Os** with properties like **1Os** with the dihydrogen chemical shift downfield of the terminal hydride resonance and a trihydride tautomer with properties like **3Re**. Thus more of the dihydrogen form of **2Os** is present in CD_2Cl_2 than in acetone-d_6 judging from the downfield shift in $\delta(H_2)$. We attempted to go to lower temperatures by use of CD_2Cl_2/Freon-12 solutions to try and directly observe resonances due to these tautomers but were hampered by solubility and resolution problems below 180 K.

Temperature-Dependent ^1H NMR Spectra Due to the Intramolecular Exchange of H Atoms between η^2-Dihydrogen and Terminal Hydride Ligands. The fluxional process which explains the spectra of complexes **1Os**, **2Os**, and **3Re** (Figures 2 and 3) is an intramolecular exchange of hydrogen atoms between the H_2 and H ligand sites.

The spectra can be simulated where two equivalent protons, A_2, in an A_2X_4 spin system with short T_2 values interchange with one proton, B, in a BX_4 spin system with a long T_2 value. This model is valid for **1Os** and **2Os** since neither complex has a large coupling $J_{AB} = |^2J(H,H_2)|$ (<1 Hz for **1Os**, ≤3 Hz for **2Os**). J_{BX} values $|^2J(H,P)|$ are obtained from the quintet at low temperature (see Table II). However J_{AX} values $|^2J(H_2,P)|$ are obtained indirectly from computer simulations since they are not resolved in the broad H_2 resonance at low temperatures. Complexes **2Os** and **3Re** give quintets in spectra at 293 K with couplings $|J(H,P)|$ of 9.4 and 17 Hz, respectively, which result from the averaging (1:2) of the terminal hydride coupling J_{BX} of −17.5 Hz for **2Os** or −21 Hz for **3Re** with a J_{AX} coupling of −5.8 Hz for **2Os** or −14 Hz for **3Re**. The J_{AX} couplings must be negative to average correctly with the negative J_{BX} couplings.[39,40] Broad singlets instead of quintets are observed in the fast exchange spectra of **1Os** up to 330 K, so that the J_{AX} value of Table II for this complex is a rough estimate from the simulation of the line widths. It should be noted that the coupling $^2J(H,P)$ is resolved in the sharp ^1H NMR resonance (1:1:1 triplet) of the H···D unit of the deuterated complex **2Os**-d_2 (see below). Such couplings to the HD ligand have been resolved for $[Ru(Cp)(dmpe)(H_2)]^+$.[12]

The chemical shift of equivalent hydrides in the fast exchange spectrum of complex **3Re** is the weighted average (2:1) of $\delta(H\cdots H)$ and $\delta(H{-}M)$. This is not true for the osmium complexes unless temperature dependences of the chemical shifts of the H_2 and H ligands are accounted for (Table II).

Spectra calculated on the basis of this information match observed spectra very well (e.g., see Figure 3). The rate constant, k, for H atoms going from the dihydrogen sites to the terminal hydride site (the rate constant for the reverse process would be $2k$) and T_2 values from the simulations are listed in Table III. Eyring plots of ln (k/T) vs $1/T$ are linear, and from them the activation parameters listed in Table IV are derived. For complex

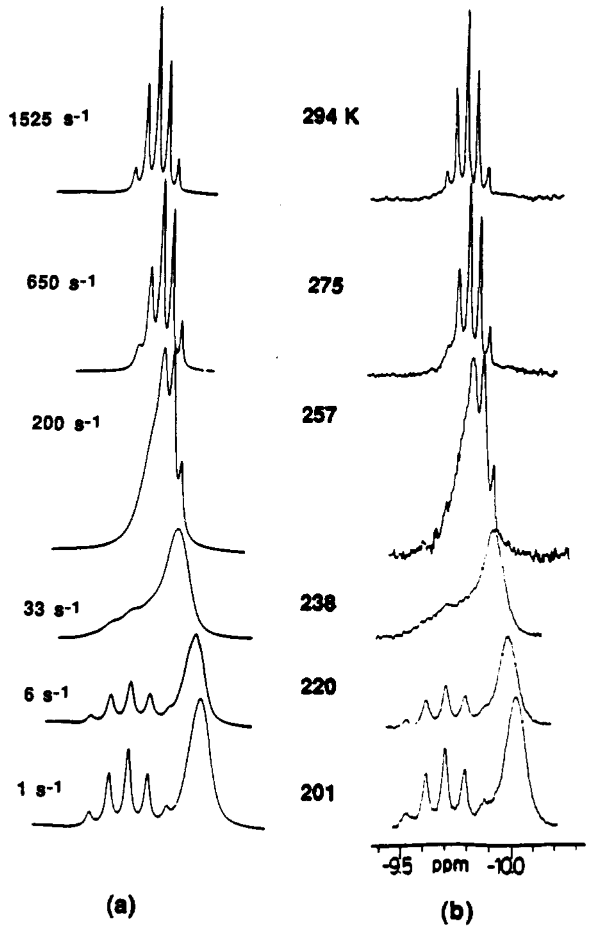

Figure 3. The simulated (a) and observed (b) 200-MHz ^1H NMR spectra in the high field region of $[Os(H\cdots H)H(depe)_2]BPh_4$, **2Os**, in acetone-$d_6$. Temperatures and rate constants for the intramolecular H-atom site-exchange process are also provided.

---

(41) Ginsberg, A. P.; Tully, M. E. J. Am. Chem. Soc. 1973, 95, 2042–2044.

Table III. T_2 Values and Rates of H Atom Exchange, k, for H Atoms Going from the Dihydrogen (H_2) Sites to the Terminal Hydride (H) Site Obtained by Line Shape Analysis[a]

complex	T, K	$T_2(H_2)$, ms	$T_1(H_2)$, ms	T_2(H), ms	T_1(H), ms	k, s^{-1}
1Os	294	59 [59]		354 [354]		830
200 MHz	276	45 [45]		270 [270]		280
CD_2Cl_2	254	30 [32]		180 [180]		50
	245		29* [28]		69* [211]	
	233	20 [20]		122 [122]		8
	225	15 [16]	19 [20]	50 [125]	136 [156]	
	215	10 [13]	17 [19]	53 [97]	[142]	
	205	12 [11]	17 [18]	66 [83]	143 [145]	
	195	7 [9]	21 [20]	49 [69]	182 [151]	0
1Os	298		90* [101*]			
400 MHz	244		49* [49*]		88* [49*]	
CD_2Cl_2	234		41* [37]		137* [280]	
	225	16 [21]	42* [37]		202* [280]	
	214	12 [18]	39 [40]	51 [135]	307 [308]	
	205	8 [15]	49 [46]		368 [355]	
	194	9 [13]	50 [59]	37 [97]	398 [456]	
1Os-d_{20}	225		21 [20]		364	
200 MHz	195		22 [20]		762	
CD_2Cl_2						
2Os	312	110		455		4100
200 MHz	294	102 [332]	420* [447]	404	420* [447]	1525
acetone-d_6	275	98		308		650
	257	78 [155]	225* [211]	229	225* [211]	200
	238	52		162		33
	220	39		107		6
	201	26 [43]	52 [50]	59	260 [213]	1
2Os	296	[140]	493* [475]		493* [475]	
400 MHz	291	144		501		1500
acetone-d_6	270	105		341		350
	248	71		218		53
	202	20 [20]	85 [80]	40	337 [340]	1
2Os	298		410* [420*]		410* [420*]	
400 MHz	201		74 [72]		202 [180]	
CD_2Cl_2	190		69 [69]		171 [170]	
	179		75 [73]		170 [182]	
	173		92 [81]		172 [201]	
3Re	273					500
200 MHz	253	35*		35*		100
CD_2Cl_2	233	35*		35*		15
	193					0
3Re	294		301* [303]		301* [303]	
400 MHz	273		238* [241]		238* [241]	
CD_2Cl_2	253		201* [197]		201* [197]	
	243		182* [184]		182* [184]	
	222		178* [176]		178* [176]	
	203		190* [204]		190* [204]	

[a] T_1 values (±5%) measured by the inversion recovery method (T_1 data for **2Os** have been reported[1]). Values in square brackets were calculated from temperature-dependent T_1 and T_2 equations as described[1] by use of the parameters listed in Table V. The values with asterisks indicate that they are averaged due to the H-atom exchange process.

Table IV. Activation Parameters in kcal mol^{-1} from the Eyring Equation for the Intramolecular Exchange of H Atoms between η^2-H_2 and Terminal H Sites[a]

complex	ΔH^*	ΔS^*	ΔG^* (300 K)
1Os	9.88	−11.5	13.3 ± 0.3
2Os	9.06	−12.9	12.9 ± 0.3
3Re	(10.6)	(−7.0)	12.7 ± 0.5

[a] The values for **3Re** are approximate.

1Os the T_2 values match those calculated by using the temperature dependence of the correlation time from the T_1 measurements in the T_2 equation.[1] For **2Os** the T_2 values from the simulations are shorter than the ones calculated from the T_2 equation;[1] an exchange process like the rapid equilibrium **1** $\rightleftarrows$ **3** could explain this broadening.

Estimates of the rates of exchange between the two equivalent hydrides and the terminal hydride in the trigonal-bipyramidal trihydride **3Re** (see Tables II and III) were also examined. Due to a limitation in the program DNMR-4, the ^2J(H,H) coupling of 9.5 Hz for **3Re** could not be included in the interchanging spin system so that the rates obtained have a greater uncertainty. Nevertheless the $\Delta G^\ddagger$ value obtained for **3Re** (Table IV) fits well in the trend that as the hydridic character of the dihydrogen ligand increases (**1Os** < **3Re**), the barrier to rearrangement decreases.

This trend supports the proposal that H-atom exchange proceeds through the fluxional rearrangements of seven-coordinate, trihydride intermediates as indicated in Scheme I. Interconversion of structures **1** → (**2**→) **3** (refer also to Figure 1) involves little motion of the P atoms although the dihydrogen must cease its rapid spinning. The exchange of H atoms occurs between structures **3** and **3′** and involves significant movement of ditertiaryphosphine P_1–P_4 as well as H_1 (or a concerted movement of both P_1–P_4 and P_2–P_3 as well as H_1). Such displacements of the P atoms would be impossible for the related complexes *trans*-$[M(H)(H_2)$(*meso*-tetraphos-1)$]^+$, M = Fe, Os, and this is why exchange is shut down by the *meso*-tetraphos-1 ligand.[32] The small $\Delta S^\ddagger$ values are in accord with an intramolecular process. A negative $\Delta S^\ddagger$ would be expected since the dihydrogen is losing its rotational degree of freedom in the trihydride intermediate. However, **3Re** also gives a negative $\Delta S^\ddagger$ value so that the activation parameters are likely determined by the energetics of movement of the ditertiaryphosphine ligands. Alternative mechanisms of site exchange are much less likely.[31] The $\Delta G^\ddagger$ value for the interconversion of six-coordinate $W(CO)_3(H_2)(P^iPr_3)_2$ to seven-coordinate $W(H)_2(CO)_3(P^iPr_3)_2$ is 16.0 kcal mol^{-1}.[24] This activation energy is somewhat larger than those of Table IV, but

Table V. The Minimum T_1 Value, T_1(min), for the Dihydrogen and Terminal Hydride Ligands (at Temperature, T(min), and Spectrometer Frequency, ν)[e]

complex	ν, MHz	T(min), K	T_1(min) H_2, ms	τ_0, ps	E_a, kcal/mol	rapid rotation r_{H_2}, Å	no rotation r_{H_2}, Å	T_1(min) M–H, s
1Os	200	205	18 ± 1	0.90	2.6	0.98	1.24	0.14
	400	233	40 ± 1	0.90	2.6	0.99	1.25	0.28
2Os	400	190	69 ± 4[a]	0.33	2.5	1.09[c]	1.37[d]	0.17[a]
	200[b]	185	40 ± 2	0.19	2.9	1.12[c]	1.40[d]	0.17
	400[b]	203	80 ± 2	0.19	2.9	1.12[c]	1.40[d]	0.34
3Re	400	230	178 ± 2	1.2	2.4		1.6–2.1	0.18

[a] Larger uncertainty due to overlap of resonances. [b] For acetone-d_6 solution. [c] Value increases to ~1.2 Å if relaxation due to depe protons is accounted for (see text). [d] Values increases to ~1.5 Å if relaxation due to depe protons is accounted for (see text). [e] Obtained by direct observation and/or fitting the data of Table III to the temperature-dependent T_1 equation with a temperature-dependent correlation time $\tau = \tau_0 e^{E_a/RT}$.[1] The H–H distance of the dihydrogen ligand, r_{H_2} is calculated for the case of rapid rotation of the dihydrogen with respect to the tumbling of the molecule and for the case of slow or no rotation. The solvent is CD_2Cl_2 except where noted.

the seven-coordinate complex in this case is thought to have a capped octahedral geometry.

The isotope effect for the rate of site exchange for **2Os** versus **2Os**-d_2 was reported as 1.4 ± 0.2.[20] The large error is due to difficulties in preparing **2Os**-d_2 free from other isotopomers and simulating exchange processes in the complex spin system (see below). More work is required before a reliable number is obtained.

^{31}P NMR Spectra. The ^{31}P NMR spectra of **1Os**, **2Os**, and **3Re** are singlets at 37.2, 41.3, and 54.8 ppm, respectively, in the temperature range 200 to 300 K. The rapid interconversion **3** → **2** → **1** → **2** → **3** (refer to Scheme I and Figure 1) with rotation of the dihydrogen in **1** would allow rapid interchange of axial (P_3, P_4) and equatorial (P_1, P_2) phosphorus atoms. This could explain the equivalence of P atoms of **2Os** and **3Re** (assuming it has an accessible dihydrogen form) to low temperatures as indicated by both the ^{31}P NMR and the quintet pattern in the ^{1}H NMR spectrum of the terminal hydride ligand. The upper bound for the activation energy of this process is estimated to be 9 kcal mol^{-1}. This corresponds to a rate of 2000 s^{-1} at 200 K.

If there is not a rapid equilibrium between **1** and **3**, then some other low-energy process must be proposed that moves separate hydrides H_1 and H_2 (see Scheme I) in **2Os** and **2Re** to render the 4 P atoms equivalent at 200 K. The mechanism must not allow interchange of H atoms with the terminal hydride, H_3, since this is stopped at 200 K.

Longitudinal Relaxation Times, T_1, of the H_2 and H Ligands. The T_1 values of the dihydrogen nuclei, $T_1(H_2)$, and the hydride ligand, T_1(H), were determined over the temperature range of 190–300 K for the complexes (Table III). A complete report of how possible H–H distances were determined for complex **2Os** has already been described.[1]

The procedure involves varying r_{HH} (the distance between the observed nucleus and the nucleus (nuclei) causing its relaxation) in the equation expressing spin–lattice relaxation by the dipolar mechanism. The parameters τ_0 and E_a of the temperature-dependent correlation time, $\tau = \tau_0 e^{E_a/RT}$, are also varied. There are two limiting cases: (1) spinning of the dihydrogen is a much higher frequency process than the tumbling of the molecule (structure **1**) and (2) the motion of the dihydride unit is slow relative to the tumbling frequency (structures **2** or **3**). Use of a suitable spectral density function for each case results in a calculated H–H distance which is a factor of 0.793 shorter for case (1) than case (2).[1] For example, the H–H distance for **2Os** is either 1.12 Å (case 1) or 1.40 Å (case 2).

When the rate of intramolecular H-atom exchange exceeds about 10 s^{-1} (Table III), then the rates of relaxation ($1/T_1$) of the H_2 and hydride nuclei start to average, with the hydride T_1 value changing much faster than that of the H_2 unit (see Table III). Above exchange rates of about 100 s^{-1} the observed relaxation rates are averages of the H_2 and hydride rates weighted 2:1. The best-fit parameters (a unique solution in each case assuming rapid spinning, a second assuming no spinning) for the complexes are found in Table V. The τ_0 and E_a parameters for the dihydrogen resonance also successfully describe the temperature dependence of the T_1 values of the terminal hydride.

Scheme I. Mechanism for the Intramolecular Exchange of H Atoms between Hydride and Dihydrogen Ligands

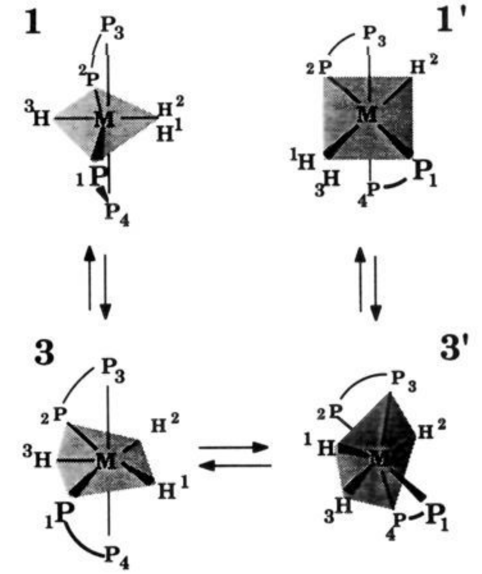

The same dihydrogen bond distance r_{H_2} (Table V) is obtained from the fit to the data or from the T_1(min) value (when it is observed) according to the procedure of Hamilton and Crabtree[4] (with the use of $\omega\tau = 0.62$ when T_1 is a minimum). The simplified equations for H–H distance calculations from T_1(min) are

$$r_{H_2} = 5.815(T_1(\mathrm{min})/\nu)^{1/6} \tag{4}$$

assuming no rotation of H_2 (r in Å, T_1 in s, ν, the spectrometer frequency, in MHz) and

$$r_{H_2} = 0.793 \times 5.815(T_1(\mathrm{min})/\nu)^{1/6} = 4.611(T_1(\mathrm{min})/\nu)^{1/6} \tag{5}$$

assuming rapid rotation of the H_2 ligand.

A long distance of 0.99 (2) Å for **1Os** is obtained assuming rapid spinning of an η^2-dihydrogen ligand. Other H atoms on the dppe ligands do not contribute significantly to the relaxation of η^2-H_2 and hence do not affect the H–H distance calculation. This is clear from T_1 measurements on the complex $[Os(H)\{P(C_6D_5)_2PCH_2CH_2P(C_6D_5)_2\}_2(\eta^2\text{-}H_2)]BF_4$, **1Os**-$d_{20}$ (Table III). There is a negligible change in the T_1 of η^2-H_2 going from **1Os** to **1Os**-d_{20} (21 → 22 ms, 400 MHz, 195 K), whereas there is a large change in the T_1 of the terminal hydride (182 → 762 ms). The analogous iron complex gave similar results.[1] These data can be used to rule out a possible rapid equilibrium between structures **1** and **2** or **3** of Figure 1 for **1Os** since the T_1 time of the H_2 unit in **3** would be greatly increased upon deuteration of the ligand; averaging of this longer T_1 time with the T_1 time of **1** would result in a T_1 value that is significantly longer than the one observed for **1Os**-d_{20}.

If the correlation time of the H_2 were not shorter than the one for the tumbling of **1Os** in solution, then the H–H distance would

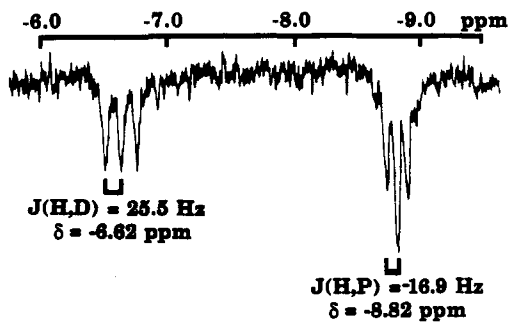

Figure 4. ^{1}H NMR spectrum at 200 MHz in the high field region of *trans*-[Os(H)(dppe)$_2$(HD)]BF$_4$ in acetone-d_6/CD$_2$Cl$_2$ (70/30 V/V) at 232 K obtained by use of an inversion recovery experiment with a delay, τ, of 10 ms to null out the η^2-H$_2$ signal of the isotopomer *trans*-[Os(D)(dppe)$_2$(H$_2$)]BF$_4$.

be 1.24 (3) Å, and **1Os** would have structure **2**, Scheme I; the observation of a large ^1J(H,D) value makes this an unlikely situation (see below). Distances in the range 1.05–1.2 Å can be ruled out since they would arise from intermediate rotation rates which give ln (T_1) vs 1/T curves with shapes characteristically different to those observed; see, for example, the curve calculated for an intermediate rotation rate of H$_2$ in [RuH(dppe)$_2$(H$_2$)]$^+$ (Figure 4 in ref 1).

Complex **2Os** has an even longer minimum value T_1(H$_2$) than **1Os** probably because the more electron-releasing depe ligands favor more hydride character in the H$_2$ unit. The H–H distance was calculated as 1.12 (3) Å assuming rapid rotation of the H$_2$ ligand (structure **1**) or 1.40 (3) Å (Table V) for the slow or no rotation case (structure **2**) assuming that the depe ligand protons do not contribute significantly to relaxation of the dihydrogen unit.[1] A third possibility is that the observed rate of relaxation, 1/T_1 (1/0.08 Hz at 400 MHz, 200 K), is actually a weighted average of rates for rapidly interconverting tautomers **1** and **2** (or **3**). The fact that rates of relaxation are consistently faster in CD$_2$Cl$_2$ than in acetone-d_6 for **2Os** (see Tables III and V) supports the δ(H$_2$) chemical shift argument (see above) that more of tautomer **1** is present in CD$_2$Cl$_2$.

The H–H distances reported for **2Os** are probably too short because the depe protons do contribute to the dihydrogen relaxation rate. This additional contribution can be approximated by use of the minimum value of the terminal hydride T_1(H) since this hydride is in a similar environment to the H$_2$ ligand (eq 6).

$$\frac{1}{T_1(\mathrm{H_2,\ obs})} = \frac{1}{T_1(\mathrm{H_2,\ true})} + \frac{1}{T_1(\mathrm{H,\ obs})} \qquad (6)$$

Complex **2Os** has T_1(H$_2$, obs) = 0.080 and T_1(H, obs) = 0.34 s at 400 MHz in acetone-d_6. The corrected minimum T_1(H$_2$, true) = 0.10 s, and the corrected H–H distances are 1.17 Å assuming rapid spinning of H$_2$ and 1.47 Å assuming no spinning. For the CD$_2$Cl$_2$ data the respective distances are 1.13 and 1.42 Å. These were calculated by use of the T_1(H, obs) value of 0.34 s which was more accurately determined in acetone-d_6 than in CD$_2$Cl$_2$.

Note that the minimum T_1 values are proportional to the frequency of the spectrometer. The T_1 value of 10 ms for the complex [Os(H)(H$_2$){P(OEt)$_2$Ph}$_4$]$^+$ measured at 80 MHz is comparable to the ones observed in this work if it is scaled up to 200 MHz (25 ms); it is not unusually short as claimed.[42]

Relaxation Rates of Hydrogen and Phosphorus Coordinated to Re. The minimum T_1 values for the resonances of the trihydride **3Re** are also included in Table V. These are slightly shorter than T_1 times of the terminal hydrides of complexes **1Os** and **2Os**.

There is a question whether the metal contributes significantly to the relaxation of coordinated hydrogen ligands.[43] To examine this we also determined the minimum T_1 value of the phosphorus nuclei (at 162 MHz) in complexes **1Os** and **3Re** (0.52 and 0.25 s, respectively). These values do parallel the minimum T_1 values of the hydrides in these complexes (0.28 and 0.18 s, respectively) which suggests that the Re has a contribution to the overall relaxation rate of coordinated H or P atoms of about 2 s^{-1} (= 1/0.18–1/0.28, 400 MHz) or 3 s^{-1} at 250 MHz. Thus the averaged relaxation rate for polyhydrides, 1/T_1(min, observed), will be faster than the one calculated, 1T_1(min, calculated), by this amount. This contribution is great enough to affect the H–H distances calculated from T_1(min) data, particularly when no close H–H distances are present. For example, observed T_1(min) values for the polyhydrides ReH$_7$(dppe) (67 ms at 250 MHz) and ReH$_5$(PPh$_3$)$_3$ (138 ms at 400 MHz)[44] are shorter than ones calculated by Crabtree (77 and 148 ms, respectively) when the effect of Re is neglected.[45] When this effect is included, the values become 67 and 115 ms, respectively. The 67-ms value, calculated from neutron diffraction positions, now agrees well, whereas the 115-ms value, calculated from X-ray determined positions, is too low. This makes sense since distances to hydrogen atoms from X-ray diffraction are usually underestimated. Relaxation contribution from Re will be twice as great for hydrides bridging between two Re atoms. Since there are four bridging hydrides in Re$_2$H$_8$(PEt$_2$Ph)$_4$, the calculated, averaged relaxation rate of 1/0.302 s^{-1} at 400 MHz based on neutron diffraction determined distances[45] has to be corrected by 3 s^{-1} (the average of four out of eight H being relaxed by two Re and four out of eight H, by one Re). This results in a calculated relaxation rate of 1/0.158 s^{-1}, in much better agreement with the observed one of 1/0.140 s^{-1}.[43] The source of the relaxation by Re is dipolar[43] since the quadrupolar mechanism has been ruled out by Crabtree.[45]

Preparation and Properties of the Deuterated Complexes. The complex **1Os**-d_1 was prepared by reacting OsH$_2$(dppe)$_2$ with HBF$_4$ in D$_2$O/diethyl ether. It is a mixture of isotopomers *trans*-[Os(H$_t$)(dppe)$_2$(HD)]$^+$ and *trans*-[Os(D$_t$)(dppe)$_2$(H$_2$)]$^+$ because of the rapid site-exchange process (the subscript t indicates trans). The coupling ^1J(H,D) of 25.5 Hz was resolved by use of an inversion recovery experiment at 232 K (Figure 4, Table VI). This relatively high value is more consistent with the H–H distance of 0.99 Å, obtained assuming rapid rotation of the H$_2$ ligand, than the longer distance of 1.24 Å (see above) and supports the idea that a "stretched" dihydrogen ligand can still spin rapidly (or the H atoms can quantum mechanically tunnel) on its binding site. The HD peaks of Figure 4 are broad enough to contain the proposed but unresolved 5-Hz coupling, ^2J(H,P) (see Table II).

The complexes **2Os**-d_1 and **2Os**-d_2 were prepared by reacting *trans*-OsClH(depe)$_2$ with HD or D$_2$, respectively, as in eq 7 (XY = HD or D$_2$). Resonances due to the various isotopomers can be assigned in the high field region of the ^{1}H NMR spectra obtained below 220 K (Figures 5 and 6, Table VI). The spectra

$$\textit{trans}\text{-M(Cl)(H)(depe)}_2 + \text{NaBPh}_4 + \text{XY} \rightarrow \textit{trans}\text{-[M(XY)(H)(depe)}_2\text{]BPh}_4 + \text{NaCl} \qquad (7)$$

for **2Os**-d_1 are complicated by the fact that H$^+$/D$^+$ exchange occurred when this complex was precipitated by using MeOH so that **2Os**-d_1 became contaminated with 20% **2Os**-d_0. MeOD was used to isolate **2Os**-d_2 so that the only contaminant in this case would be **2Os**-d_3. As reported earlier, exchange of H$^+$/D$^+$ between isotopomers is very slow in acetone-d_6 in the absence of alcohol.[20]

In spectra of *trans*-[Os(H···D)(D$_t$)(depe)$_2$]$^+$ obtained at 220 K in acetone-d_6, the J(H···D) coupling was partially resolved (Figure 5a) and found by simulation to be 10.5 ± 0.1 Hz. The ^2J(H,P) coupling of −5.4 ± 0.1 Hz was also partially resolved. This is a similar value to the one deduced for **2Os**-d_0. At temperatures lower than 220 K, these couplings could not be resolved because T_2 becomes too short; at temperatures higher than this the site exchange process causes line broadening and reduction of the HD coupling constant. Under similar conditions but with CD$_2$Cl$_2$ as the solvent, the J(H···D) coupling for **2Os**-d_2 when the solvent is changed (Figure 5c) was found by simulation to be 11.4

---

[42] Antoniutti, S.; Albertin, G.; Amendola, P.; Bordignon, E. *J. Chem. Soc., Chem. Commun.* **1989**, 229–230.

[43] Cotton, F. A.; Luck, R. L.; Root, D. R.; Walton, R. A. *Inorg. Chem.* **1990**, *29*, 43–47.

[44] Cotton, F. A.; Luck, R. L. *J. Am. Chem. Soc.* **1989**, *111*, 5757–5761.

[45] Crabtree, R. H. *Acc. Chem. Res.* **1990**, *23*, 95–101.

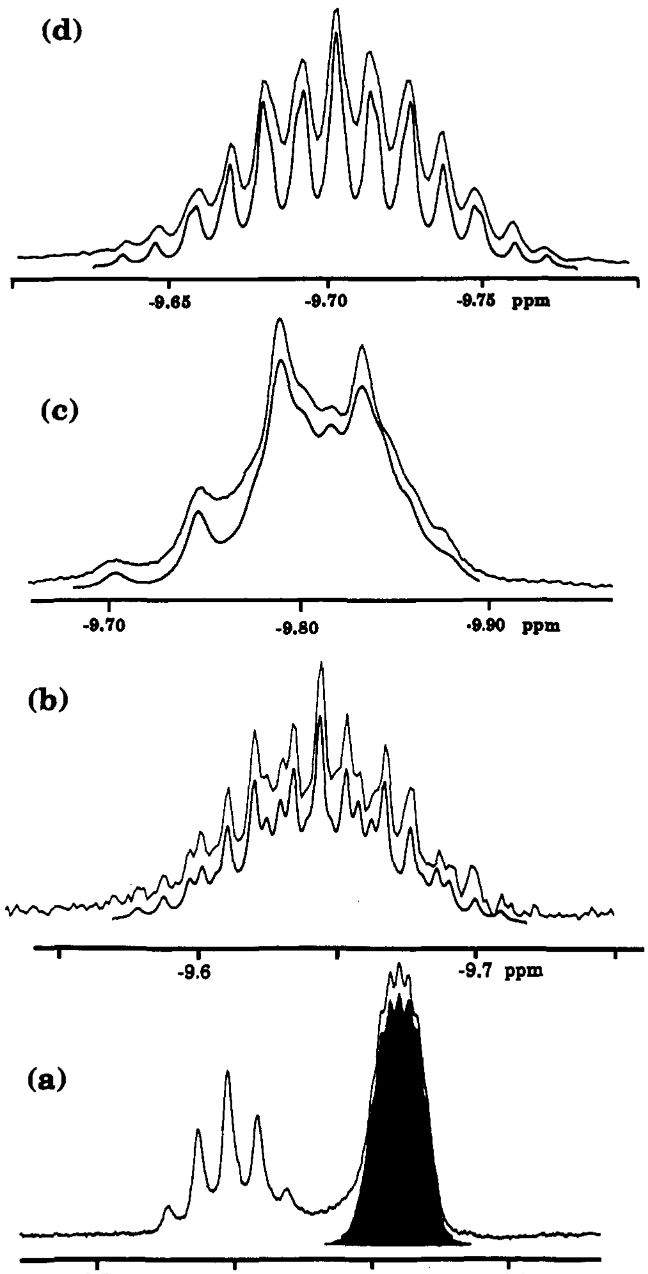

Figure 5. (a) ^{1}H NMR spectrum in the high field region at 400 MHz and 220 K of **2Os**-d_2 in acetone-d_6. The black triplet of quintets of the H···D unit (T_2 = 0.05 s) was calculated based on J(H,D) = 10.5 Hz, ^2J(H,P) = −5.4 Hz. (b) ^{1}H NMR spectrum at 325 K of **Os**-d_2 in acetone-d_6. The simulated spectrum (traced below) was calculated based on |J(H,D)| = 3.80 ± 0.05 Hz and |^2J(H,P)| = 9.40 ± 0.05 Hz, T_2 = 0.2 s. (c) ^{1}H NMR spectrum in the high field region at 400 MHz and 220 K of **2Os**-d_2 in CD_2Cl_2: J(H,D) = 11.4 ± 0.4 Hz, ^2J(H,P) = −5.0 Hz, T_2 = 0.05 s. (d) ^{1}H NMR spectrum at 311 K of **Os**-d_2 in CD_2Cl_2: |J(H,D)| = 4.10 ± 0.05 Hz and |^2J(H,P)| = 9.30 ± 0.05 Hz, T_2 = 0.2 s.

± 0.4 Hz. The increase in this coupling is further evidence that there is more of the η^2-H_2 (or η^2-HD) tautomer in CD_2Cl_2 than in acetone-d_6. Integrations and simulations of the spectra always give the statistical 1:2 ratio of protons between terminal hydride and η^2-HD sites indicating that hydrogen has no preference between sites in this case.

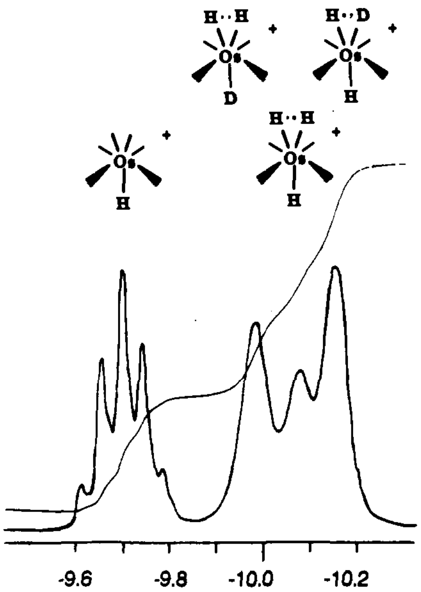

Figure 6. ^{1}H NMR spectrum in the high field region at 400 MHz and 200 K of 80% **2Os**-d_1 with 20% **2Os**-d_0 in acetone-d_6.

Above 300 K the pattern for **2Os**-d_2 becomes a quintet of 1:2:3:2:1 quintets (due to coupling to two equivalent deuteria with I = 1) (Figure 5b,d). The averaged ^2J(H,P) coupling of −9.4 Hz (0.333 × −17.5 + 0.666 × −5.4) is observed and this indicates that the isotopomers *trans*-$[Os(H\cdots D)(D_t)(depe)_2]^+$ and *trans*-$[Os(D\cdots D)(H_t)(depe)_2]^+$ are in the expected statistical ratio of 2:1 and that H shows no significant preference for either the terminal hydride (H_t) or HD sites. For the acetone-d_6 case, the observed coupling J(H,D) = 3.8 Hz results from the averaging of couplings for *trans*-$[Os(H\cdots D)(D)L_2]^+$ {0.5 × J(H···D) + 0.5 × ^2J(H,D) = 0.5 × 11.4 + 0.5 × 0.0 = 5.74 Hz} and for *trans*-$[Os(D\cdots D)(H)L_2]^+$ {2 × ^2J(H,D) = 0.0 Hz} which must be weighted according to the statistical abundance ratio of 2:1 (0.666 × 5.74 + 0.333 × 0.0 = 3.8 Hz) (see Figure 5b). Thus J(H···D) must be 11.4 Hz at 325 K in acetone-d_6, slightly increased from the value of 10.5 Hz found at 220 K. Again corresponding J(H···D) values are larger in CD_2Cl_2 than in acetone-d_6 (Table VI); at 311 K, J_{av}(H,D) = 4.1 Hz so that J(H···D) must be 12.3 Hz when CD_2Cl_2 is the solvent.

The observation of a small H-D coupling in the fast-exchange spectra is important, and this appears to be the second such report. A study by Bampos and Field reported a J(H,D) value of 10 Hz.[46] This is the value expected for rapid intramolecular exchange of H/D atoms in the HD_2 isotopomer of the *cis*-η^2-dihydrogen-hydride complex $[FeH\{P(CH_2CH_2CH_2PMe_2)_3\}(\eta^2\text{-}H_2)]^+$ where the ^1J(H,D) value for the η^2-HD ligand is actually 30 Hz (0.333 × 30 + 0.666 × 0.0). *Our work suggests that three nuclei (H, D, D) do not have to retain bonds between themselves to give an averaged J(H,D) coupling.*

Although resonances for the various isotopomers of **2Os**-d_1 could be resolved (Figure 6), no J(H,D) triplets were resolved. Simulation of the HD resonances with ^2J(H,P) = 5 Hz suggest that J(H··D) is ca. 11 Hz. The large chemical shift difference (0.07 ppm) between δ(H···H) and δ(H···D) of the two isotopomers of **2Os**-d_1 results from the higher trans influence of the deuteride trans to the H···H unit than the hydride trans to the H···D unit.[47] *This is the first report of the high trans influence of deuterium on chemical shifts in a dihydrogen complex.* The hydride resonances for **2Os**-d_1 coalesce in an interesting way as the temperature is raised because of intramolecular H atom exchange between $[Os(H\cdots H)(D)L_2]^+$ and $[Os(H\cdots D)(H)L_2]^+$ forms. The resonances at −10.1 (H···D, Table VI), −9.93 (H···H), and −9.7 ppm (Os(H)) broaden at 240 K and then sharpen at 293 K to a multiplet at −9.73 ppm which is also the hydride chemical shift of $[Os(H\cdots H)(H)L_2]^+$ at this temperature (Table II).

The chemical shift of the H_2 and HD ligands in the isotopomers of **2Os**-d_1 and **2Os**-d_2 have temperature dependences (Table VI) similar to that of the H_2 in **2Os**-d_0 (Table II).

The ^{1}H NMR spectra of the complex **3Re**-d_2 are identical with those of the all proton complex. Thus no J(H,D) coupling or

---

[46] Bampos, N.; Field, L. D. *Inorg. Chem.* **1990**, *29*, 587–588.

[47] Crabtree, R. H.; Habib, A. *Inorg. Chem.* **1986**, *25*, 3698–9.

Table VI. ^{1}H NMR Chemical Shifts of the Isotopomers of **1Os** (at 200 MHz) and **2Os** (at 400 MHz) in Acetone-d_6 (or CD_2Cl_2 Where Specified)

complex, T, K	δ(HD or H_2)	J(H,D)	^2J(H,P)	δ(H)	^2J(H,P)
1Os-d_1, 232					
$[Os(HD)(H)L_2]^+$	−6.62 t	25.5	<|5|	−8.82 q	−16.9
$[Os(H_2)(D)L_2]^+$	−6.61 br				
2Os-d_1, 200					
$[Os(HD)(H)L_2]^+$	−10.10 br[a,c]	≤12	∼−5	−9.68 q	−17.5
$[Os(H_2)(D)L_2]^+$	−9.93 br[b,c]				
2Os-d_2, 200					
$[Os(HD)(D)L_2]^+$	−10.02 m[d]	10.5 ± 0.1	−5.4		
$[Os(D)_2(H)L_2]^+$				−9.70 q	−17.5
2Os-d_2, 325					
$[OsHD_2L_2]^+$	−9.64 m	3.80 ± 0.05	−9.40 ± 0.05	−9.64 m	−9.40 ± 0.05
2Os-d_2, 220[e]					
$[Os(HD)(D)L_2]^+$	−9.81 m	11.4 ± 0.4	−5.0		
$[Os(D)_2(H)L_2]^+$				−9.79 q	−17.8
2Os-d_2, 311[e]					
$[OsHD_2L_2]^+$	−9.70 m	4.10 ± 0.05	−9.30 ± 0.05	−9.64 m	−9.30 ± 0.05
2Os-d_3, 200[f]					
$[Os(D)_2(D)L_2]^+$	−10.0 br			−9.6 br	

[a] Temperature dependent, $\delta(HD) \sim 0.0028T - 10.66$. [b] $\delta(H_2) \sim 0.0028T - 10.49$. [c] The assignment of these two resonances may be reversed. [d] $\delta(HD) = 0.0034T - 10.7$. [e] CD_2Cl_2. [f] ^{2}H NMR.

Table VII. Selected Electrochemical and Infrared Properties of the Complexes *trans*-$[M(H)(ditertiaryphosphine)_2(L)]^{n+}$

		infrared[b]	
complex	electrochemistry[a] L = H_2 or $(H)_2$ E_a,[c] V	L = CO ν(CO), cm^{-1}	L = N_2 $\nu(N_2)$, cm^{-1}
$[Os(H)(dppe)_2(L)]^+$	1.15 ± 0.03 (**1Os**)	2003[d]	
$[Os(H)(depe)_2(L)]^+$	1.00 ± 0.03 (**2Os**)	1974[e]	2136[e]
$Re(H)(dppe)_2(L)$	−0.40 ± 0.03[f] (**3Re**)	1845[g]	2006[g]

[a] Versus $FeCp_2/FeCp_2^+$, CH_2Cl_2 solvent unless otherwise noted, 0.2 M n-Bu_4NBF_4 (Bu_4NPF_6 for **1Os**), 50 mV s^{-1} scan rate. [b] Nujol mull unless otherwise noted. [c] Anodic peak potential of irreversible wave; **2Os** also gives E_a = 0.6 V for BPh_4^-/BPh_4 oxidation. [d] CH_2Cl_2 solvent. [e] Reference 34. [f] THF solvent; 0.19 V versus Ag/AgCl.[64] [g] Reference 55.

isotopic perturbation of resonance is observed in the case of the isotopomers of this trihydride.

Electrochemistry and Infrared Data. Complexes **1Os** and **2Os** are difficult to oxidize and display an anodic wave at $E_a \sim 1$ V vs $FeCp_2/FeCp_2^+$ (Table VII). The cathodic return wave is very broad and likely involves the reduction at the Pt electrode of protons produced in the oxidation reaction. The E_a values give no evidence of structural differences between **1Os** and **2Os**. Removing one positive charge from **1Os** effectively gives a complex like **3Re**, which is easier to oxidize by about 1.4 V (Table VII). The infrared data for the corresponding carbonyl and dinitrogen complexes (Table VII) reflect the electrochemical behavior of the $[MHL_2]^{n+}$ binding sites: the reducing ability of the complex increases in the order **1Os** < **2Os** < **3Re**, while the CO and NN stretching frequencies decrease in the order **1Os** > **2Os** > **3Re** as expected from backbonding considerations.[48]

Discussion

Complex **1Os** contains a rapidly spinning, strongly coordinated dihydrogen ligand with an H–H distance of 1.0 Å which is significantly longer than the H–H distance of 0.82 Å of $[Fe(H)(dppe)_2(\eta^2-H_2)]^+$ obtained by neutron diffraction. In general 5d metal–ligand σ bonds are thought to be about 10 kcal mol^{-1} greater than 3d metal complexes (5 kcal mol^{-1} greater than 4d).[49] This greater σ contribution to the bonding likely explains the lengthening of the H–H bond and the increased $Os-H_2$ bond energy; arguments based on increased backbonding are less convincing because the analogous iron complex has much higher energy d electrons.[31] **1Os** is less reducing than **2Os** and much less than **3Re**. It is for this electronic reason that less electron-releasing **1Os** does not oxidatively add the H–H bond. Other periodic trends in the properties of dihydrogen complexes will be reported elsewhere.[31]

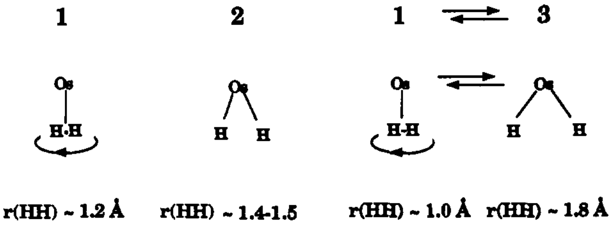

Figure 7. Three possible structures for the dihydrogen unit in **2Os** and the other unusual osmium complexes of Table VIII.

The presence of chelating ligands is not essential to give a dihydrogen complex like **1Os**. When monodentate phosphorus donors have small cone angles and are not too electron-donating (i.e., $P(OEt)_3$ ligands), then complexes *trans*-$[MHL_4(\eta^2-H_2)]^+$, M = Fe, Ru, Os, can form.[50] $[OsH_3(PPh_3)_4]^+$ is not a dihydrogen complex[14] because octahedral *trans*-$[OsH(H_2)(PPh_3)_4]^+$ could not form because of steric repulsion between PPh_3 ligands (no regular octahedral complexes containing four PPh_3 ligands are known).

Figure 7 presents three possible structures for **2Os** in solution at 200 K and for the other Os complexes of Table VIII with J(H,D) < 25 Hz. Structure **1** with a spinning dihydrogen ligand has been assumed to be the structure of such complexes.[1,10,13,14,15,19,20,32,48] The following evidence supports this: the low T_1 time of the H_2 unit, the small ^2J(H,P) and ^2J(H,H) coupling constants, the "medium size" J(H,D), and the possible observation of ν(H–H) at 2231 cm^{-1} for $[OsH_2(NH_3)_5]^{2+}$.[13] The last observation is confused by the fact that $[Os(H)_2(en)_2]^{2+}$ also shows stretches in this region assigned to ν(OsH).[51] The evidence against structure **1** is the low lability of H_2 in these complexes and the inconsistent frequency ν(OsH) of **2Os** (see above). A plot of J(H,D) versus distances r(H,H) (from neutron or T_1 studies assuming rapid internal "spinning" of an intact H_2, Figure 8) indicates that J(H,D) would drop in a linear fashion to less than 1 Hz at $r(H-H) \sim 1.25$ Å. This is inconsistent with the fact that hydrides 1.65 Å apart (neutron) in $[IrCpH_3(AsPh_3)]^+$ give J(H,D) = 4 Hz (Table VIII) assuming that the observed J(H,T) coupling of 24–29 Hz can be related to J(H,D) by magnetogyric ratios.[22] Note that a related Os complex with no H–H bonding, $Os(\eta^5-C_5Me_5)(H)_3(CO)$,[52] shows an H–H coupling of 8.9 Hz and thus an expected HD coupling of 1.4 Hz. A single form of **2Os** with

---

(48) Morris, R. H.; Earl, K. A.; Luck, R. L.; Lazarowych, N. J.; Sella, A. *Inorg. Chem.* **1987**, *26*, 2674–83.

(49) Tilset, M.; Parker, V. D. *J. Am. Chem. Soc.* **1989**, *111*, 6711–6717.

(50) Amendola, P.; Antoniutti, S.; Albertin, G.; Bordignon, E. *Inorg. Chem.* **1990**, *29*, 318–324.

(51) Malin, J.; Taube, H. *Inorg. Chem.* **1971**, *10*, 2403–2406.

(52) Graham, W. A. G.; Hoyano, J. K. *J. Am. Chem. Soc.* **1982**, *104*, 3722–3723.

Table VIII. T_1(min, 200 MHz) and ^1J(H,D) NMR Data for Some Dihydrogen and Hydride Complexes and an Approximate Ordering of Calculated or Observed H–H Distances: r(H–H) for η^2-H_2 or r(H$\cdots$H) for Separate Hydrides

complex	T_1(min), ms	r(H–H), Å	r(H$\cdots$H), Å	^1J(H,D), Hz	ref
$W(H_2)(CO)_3(P^iPr_3)_2$	4	0.82[a]		33.5	65
$[Fe(H)(dppe)_2(H_2)]^+$	8.5	0.86		32	1
$[Ru(H)(dppe)_2(H_2)]^+$	10	0.89		33	1
$[IrH(bq)(H_2)(PPh_3)_2]^+$	7	0.92[b]		29.5	4
$[Co(H_2)(PP_3)]^+$	12.7	0.92[c]		27.8	2
$[Os(H)(\text{meso-tet})(H_2)]^+$	15.5	0.95[c]		26	32
1Os	20	1.0[c]		25.5	this work
$[OsH_2(OAc)(PPh_3)_2]^+$	21	1.0[c]	1.26[d]	14	14
$[Os(H)(H_2)(dedpe)_2]^+$	30	1.06[c]	1.34[d]	19	10
2Os	40	1.2	1.5	11	this work
$OsH_2(OEP)$	55	1.18[c]	1.48[d]	12	15
$[OsH_2(NH_3)_5]^{2+}$				15	13
$[IrCpH_3(AsPh_3)]^+$	(86)[e]		1.65[a]	4	22
3Re	90		>1.6[f]	0	this work

[a] Neutron diffraction. [b] Solid-state NMR Value. [c] From eq 6; rapid spinning of H_2. [d] From eq 5; separate hydrides. [e] May not be minimum value. [f] Longer than calculated (eq 5) since Re dipole and ligand protons contribute to the relaxation rate.

Table IX. The Postulated Properties of the Dihydrogen–*trans*-Hydride {$Os(H_2)(H_t)$} and Dihydride–*trans*-Hydride {$Os(H)_2(H_t)$} Tautomers of **2Os** and Their Averaged Properties Depending on the Temperature and the Solvent

property	separate tautomers		rapid equilibrium in acetone-d_6					rapid equilibrium in CD_2Cl_2				
	$Os(H_2)(H_t)$	$Os(H)_2(H_t)$										
T, K			203		293			190		293		
K_{eq}[h]			0.54		0.69			0.64		0.75		
$(H_2)(H_t)$:$(H)_2(H_t)$	1:0	0:1	0.35:0.65		0.41:0.59			0.39:0.61		0.43:0.57		
			calc	obs	calc	av[a]	obs	calc	obs	calc	av[a]	obs
$\delta(H_2)$, ppm	−8.8	−10.6	−9.97	−10.0	−9.86	−9.80	−9.78	−9.90	−9.88	−9.83	−9.82	−9.75
$\delta(H_t)$, ppm	−9.7[b]	−9.7[b]	−9.70	−9.70	−9.7			−9.80	−9.82	−9.80		
$^2J(H_2,P)$, Hz	0	−9	−5.7	∼−5.5	−5.3	−9.4	−9.5	−5.5		−5.1	−9.3	−9.5
$^2J(H_t,P)$, Hz	−18	−17.5	−17.7	−17.5	−17.7			−17.7	−17.7	−17.7		
$T_1(H_2)$, ms	39[c]	200[c]	82	80[c]	326[d]	435	500	76	70[c]	330[f]	444	410
$T_1(H_t)$, ms	200[c]	400[c]	300	340[c]	1300[d]			280	170[e]	1315[f]		
	$Os(HD)(D_t)$/ $Os(DD)(H_t)$	$Os(H)(D)(D_t)$/ $Os(D)_2(H_t)$										
T, K			220		325			220		311		
K_{eq}[h]			0.64		0.75			0.72		0.85		
(HD):(H)(D)	1:0	0:1	0.39:0.61		0.43:0.57			0.42:0.58		0.46:0.54		
			calc	obs	calc	av[a]	obs	calc	obs	calc	av[a]	obsd
δ(HD) of HDD_t, ppm	−8.72	−10.58	−9.86	−9.93	−9.78	−9.73	−9.7	−9.80	−9.82	−9.72	−9.73	−9.70
$\delta(H_t)$ of D_2H_t, ppm	−9.68[g]	−9.68[g]	−9.68	−9.68	−9.68			−9.78	−9.79	−9.78		
^1J(H,D) of HDD_t	27	0	10.5	10.5	11.6	3.9	3.8	11.3	11.4	12.4	4.1	4.1
^2J(H,D) of HDD_t	0	0	0	0	0			0	0	0		
^2J(H,D) of DDH_t	0	0	0	0	0			0	0	0		
^2J(HD,P)	0	−9	−5.5	−5.4	−5.1	−9.4	−9.4	−5.2	−5	−4.9	−9.2	−9.3
$^2J(H_t,P)$ of DDH_t	−18	−17.5	−17.7	−17.6	−17.7			−17.7	−17.9	−17.7		

[a] Value averaged because of rapid exchange of H_2 and H_t hydrogens at this temperature. [b] $\delta(H_t)$ is −9.8 in CD_2Cl_2. [c] Minimum T_1 values at approximately 200 K. [d] Calculated by using the temperature-dependent T_1 equation[1] and the parameters $\tau_0 = 0.19$ ps, $E_a = 2.9$ kcal mol^{-1} (see Table V). [e] Large error may be due to overlap of resonances. [f] Calculated using the temperature-dependent T_1 equation[1] and the parameters $\tau_0 = 0.33$ ps, $E_a = 2.5$ kcal mol^{-1} (see Table V). [g] $\delta(H_t)$ is 9.78 in CD_2Cl_2. [h] K_{eq} refers to $[Os(H)_2(H_t) \rightleftarrows [Os(H_2)(H_t)]$.

a spinning dihydrogen ligand provides no explanation for the solvent and temperature dependence of the H–D coupling constant and thus is considered unlikely.

Since couplings J(H,D) can range from 34 to 4 Hz as r(H$\cdots$H) increases from 0.8 to 1.65 Å, the "medium size" couplings for the osmium complexes of Table VIII suggest that there are *two closely spaced hydrides* (1.4–1.5 Å apart) in a seven-coordinate complex which is close to being octahedral (**2**, Figures 1 and 7). Other evidence for separate hydrides is the low lability of the H_2 unit, the lack of preference of H between sites in **2Os**-d_2, the infrared pattern of **2Os** (Table I), and P–Os–P angles from the X-ray study. A continuous trend in the plot of J(H,D) against r(H,H) (Table VIII, Figure 8) emerges if r(H,H) are calculated assuming rapid internal "spinning" of an intact H_2 with H–H distances between 0.8 and 1.1 Å (eq 5 used) and then no spinning for distances greater than 1.1 Å (eq 4 used). Eisenstein and Jackson have pointed out that any hydride–hydride distance is possible because hydride–hydride interactions are always attractive.[53] The variability of the H–D coupling could arise if the complex is readily deformed by solvation so that the distance between adjacent H and D ligands decreases on going from acetone to CH_2Cl_2 solvent. The T_1 times would also decrease in the observed fashion as adjacent hydrides move closer to each other. However structure **2** does not explain why the $^2J(H_2,P)$ and $^2J(H_2,H)$ couplings are so small in **2Os**, why the P atoms are all equivalent to 200 K, why the NMR parameters are temperature-dependent, and why a possible ν(H–H) has been observed for $[OsH_2(NH_3)_5]^{2+}$.[13] Note that $^2J(H_2,H)$ is 10 Hz for **3Re** (Table II) yet $^2J(H_2,H)$ must be less than 3 Hz for **2Os**.

Hydrides 1.3–1.7 Å apart might undergo quantum mechanical exchange coupling (QEC).[21] However the Os complexes described here have two equivalent protons, and so anomalous ^1H–^1H coupling constants are not observed. The QEC is likely to be quenched for HD isotopomers, and so the observed J(H,D) values of 10–14 Hz for the unusual Os complexes are likely to be scalar NMR coupling constants. QEC does not appear to result in unusually short T_1 times for the hydrides judging from a reasonably long value of 210 ms for $[IrCpH_3(AsPh_3)]^+$ at 490 MHz, 178 K.[54]

---

(53) Jackson, S. A.; Eisenstein, O. *J. Am. Chem. Soc.* **1990**, *112*, 7203–7207.

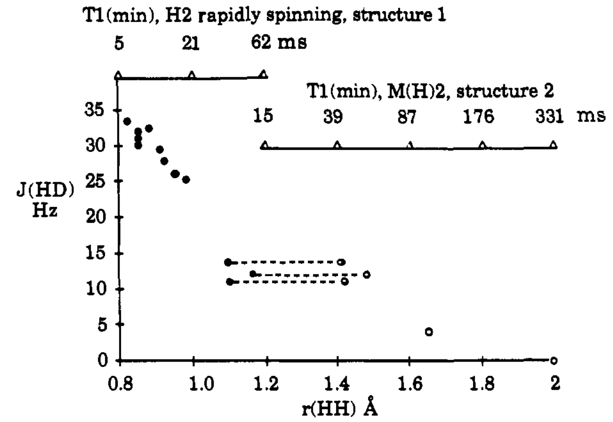

Figure 8. Plot of J(H,D) in Hz for an isotopomer containing adjacent H and D nuclei versus the separation between the nuclei, r(HH), in Å, as determined by NMR or diffraction methods (see Table VIII). Also shown are nonlinear scales for T_1(min) values at 200 MHz which are related to the distance scale, r(HH), by eq 5 for the separate hydrides $M(H)_2$ (empty circles) and by eq 6 for the "spinning" η^2-H_2 case (filled circles). Note that HD gas has J(H,D) of 43 Hz and r(H–D) of 0.74 Å.

An alternative explanation for the small coupling J(H,D) is *a rapid equilibrium between dihydrogen and dihydride tautomers* where **2Os** has properties (coupling constants to the H_2 unit, relaxation rates, chemical shifts) averaged between those expected for structures **1** and **3** in Figure 7. The interconversion has to be so rapid that spectra are in the fast-exchange limit even at 180 K. The solution infrared data suggest **2Os** is mainly in the trihydride form. The trihydride tautomer, $Os(H)_2(H_t)$, should have $r(H\cdots H) \sim 1.8$ Å, $T_1(\text{min}, H_2) \sim 200$ ms, and $J(H,D) \sim 0$ Hz, like **3Re**. This is assumed to be rapidly interconverting with an $Os(H_2)(H_t)$ tautomer, like **1Os** with structure **1**. This tautomer should have $r(H-H) \sim 0.99$ Å, $T_1(\text{min}, H_2) \sim 39$ ms, $^1J(H,D) \sim 27$ Hz, and the chemical shift difference $[\delta(H_t) - \delta(H_2)] \sim 2$ ppm with $\delta(H_2)$ downfield of $\delta(H_t)$. See Table IX for a complete listing of properties of these two tautomers. The proportion of **1**:**3** at 200 K should then be about 0.4:0.6 to give the observed J(H,D) coupling of ~11 Hz. The fact that averaging of J(H,D) values occurs for the intramolecular site-exchange process described above supports the proposal that J(H,D) values will also average (instead of decouple) in the case of a rapid equilibrium.

Sensible equilibrium constants can be obtained based on these reasonable properties of the tautomers that explain the temperature dependence of the chemical shifts, T_1 values, and J(H,D) coupling constants (Table IX). As the temperature increases, K_{eq} for the process $\{Os(H)_2(H_t)\} \rightleftarrows \{Os(H_2)(H_t)\}$ increases ($\Delta H \sim 0.3$ kcal mol^{-1}, $\Delta S \sim 0.3$ eu in acetone-d_6, $\Delta H \sim 0.2$ kcal mol^{-1}, $\Delta S \sim 0.2$ eu in CD_2Cl_2). Crabtree has reported a similar result for the equilibrium $[ReH_4(CO)(PMe_2Ph)_3]^+ \rightleftarrows [ReH_2(H_2)(CO)(PMe_2Ph)_3]^+$, also with K_{eq} less than one.[45] On the other hand, the equilibrium $WH_2(CO)_3(PR_3)_2 \rightleftarrows W(H_2)(CO)_3(PR_3)_2$ with $K_{eq} > 1$ has negative ΔH and ΔS values.[24] The data in Table IX also indicate that there is an equilibrium isotope effect where deuterium substitution of **2Os** results in an increase in K_{eq} and hence a favoring of the $(\eta^2\text{-HD})(D_t)/(\eta^2\text{-}D_2)(H_t)$ species over the (H)(D)(H) forms.

The rapid equilibrium also explains why the P atoms in **2Os** are equivalent to low temperature and why two forms may be present in the solid state (X-ray, IR evidence). The interconversion is accessible by a slight movement of the phosphine ligands (Figure 1) and is estimated to have $\Delta G^\ddagger \leq 9$ kcal mol^{-1}. This energy barrier is lower than those of other dihydrogen–dihydride equilibria (12–16 kcal mol^{-1})[12,23-25] where the complexes likely undergo larger changes in geometry.

3Re is a trihydride since three separate hydrides are more effective at removing electron density from the electron-rich metal (see Table VII) than a dihydrogen and a hydride ligand. Dihydrogen is not readily lost from **3Re**, and CO does not react with solutions of **3Re** at 20 °C. If $ReH(dppe)_2$ is generated thermally or photochemically, it rapidly oxidatively inserts into an H–H or C–H bond[55] to bring down the energy of its 5d electrons. $[OsH(depe)_2]^+$ is expected to have low-lying 5d electrons and shows no propensity to insert into C–H bonds; no incorporation of D into the depe or dppe ligands of complexes **1Os**-d_1 or **2Os**-d_2 has ever been detected by D NMR.

Conclusions

The novel solvent and temperature-dependent J(H,D) coupling constant and other properties of **2Os** indicate that homolytic cleavage of H_2 in **2Os** is a low-energy process where a (spinning-dihydrogen)(hydride) form and a trihydride tautomeric form are interconverting rapidly, even at 180 K. This is the first report of a variable J(H,D) coupling constant for an HD complex. However, we are unable to rule out the possibility that **2Os** is an unusual trihydride with a short hydride-to-hydride distance ranging between 1.4 and 1.5 Å depending on the solvent and temperature. Other notable features of the spectra of the isotopomers of **2Os** are the larger trans influence of deuteride than hydride on the HD chemical shift and the observation of an averaged H–D coupling of ~4 Hz at 293 K in the fast-exchange limit of the intramolecular $(HD)(D_t) \rightleftarrows (D_2)(H_t)$ interchange process.

1Os is a true η^2-dihydrogen complex, whereas there is complete homolytic cleavage of H_2 in the trihydride **3Re**. The more electron-donating depe ligand changes the properties of **2Os** versus **1Os** considerably so that a seven-coordinate, Os(IV) trihydride tautomer becomes slightly more stable than the six-coordinate Os(II) dihydrogen(hydride) form. For the trihydride form of **2Os** the gain in Os–H σ bond energy must outweigh the loss in H–H bond energy (which is weakened in this case by $d\pi \rightarrow \sigma^*$ back-donation) and the destabilization due to repulsion between bonding electrons to ligands around the seven-coordinate Os.

Several η^2-HD complexes have been reported to give low (<25 Hz) J(H,D) coupling constants. The temperature and solvent dependence of these couplings should be examined. It is possible that all the Os complexes in Table VIII with isotopomers with $J(H,D) < 20$ Hz have a substantial fraction of a dihydride tautomer in equilibrium with a dihydrogen complex with $r(H-H) \sim 1.0$ Å ($J(H,D) \sim 27$ Hz). A small fraction of η^2-H_2 form of a polyhydride complex like $ReH_7(PPh_3)_2$ which rapidly averages with the "classical form" could explain the dichotomy of properties reported.[56] The interpretation of T_1 data as a function of temperature can also be complicated by such a fast-exchange process as it was for the case of **2Os**. The reports of anomalous line broadening of the dihydrogen resonance[1] might also be explained by this process.

Clearly the criterion for stable dihydrogen binding sites—those that have $\nu(N_2)$ in the range 2060–2180 cm^{-1} for corresponding dinitrogen complexes[48]—cannot reliably predict the mode of H–H bonding for 5d metals. Exceptions to the rule are complexes likely to have both dihydrogen and dihydride forms in rapid equilibrium where corresponding dinitrogen complexes $[OsH(depe)_2(N_2)]^+$,[34] $OsOEP(N_2)(THF)$,[15] $[Os(N_2)(NH_3)_5]^{2+}$,[13] and $ReCl(N_2)(PMePh_2)_4$[16] have $\nu(N_2)$ = 2136, 2030, 2010, and 1925 cm^{-1}, respectively. Neutron diffraction must also play a key role in determining the structure of such hydrides in the transition region between dihydrogen and dihydride.

Experimental Section

Unless otherwise noted, all manipulations were done in an Ar or H_2 atmosphere by use of Schlenk techniques. Solids were handled in a Vacuum Atmosphere drybox under N_2. All solvents were dried over appropriate reagents[57] and distilled under N_2 before use. D_2 was obtained from Matheson Gas Products. Phosphines ligands were purchased from Strem Chemical Co. or Digital Speciality Chemicals Ltd. [Os_2Cl_3-

---

(54) Heinekey, D. M.; Payne, N. G.; Schulte, G. K. *J. Am. Chem. Soc.* **1988**, *110*, 2303–2305.

(55) Bradley, M. G.; Roberts, D. A.; Geoffroy, G. L. *J. Am. Chem. Soc.* **1981**, *103*, 379–384.

(56) Luo, X.; Crabtree, R. H. *Inorg. Chem.* **1989**, *28*, 3775–3777.

(57) Perrin, D. D.; Armarego, W. L. F.; Perrin, D. R. *Purification of Laboratory Chemicals*; Pergamon: Toronto, 1980.

$(PEtPh_2)_6]Cl\cdot 2H_2O$ and $[Os_2Cl_3(PEt_2Ph)_6]Cl$ were prepared by the method described by Chatt and Hayter.[58] $OsCl_2(dppe)_2$, $OsCl_2(depe)_2$,[58] and $OsClH(depe)_2$ {IR $\nu(OsH) = 2053$ cm^{-1} (Nujol mull); Chatt and Hayter report $\nu(OsH) = 2038$ cm^{-1}}[59] were prepared as described. $P(C_6D_5)_2CH_2CH_2P(C_6D_5)_2$, dppe-$d_{20}$, was prepared as reported,[1] and *cis*-$OsCl_2(dppe\text{-}d_{20})_2$ was prepared by using the Chatt method[58] but substituting dppe-d_{20} for dppe. Infrared spectra were recorded with a Nicolet 5DX FTIR spectrometer as Nujol mulls on NaCl plates or in the stated solvent in 0.1 mm KBr solution cells. NMR spectra were obtained on a Varian XL-400, operating at 400.00 MHz for ^1H, 161.98 MHz for ^{31}P, or on a Varian XL-200 operating at 200.00 MHz for ^1H, 80.98 MHz for ^{31}P. Some variable-temperature ^{31}P NMR and selective hydride decoupling experiments were carried out by use of the Bruker WP400 spectrometer at the South Western Ontario Regional NMR facility. Chemical shifts refer to room temperature conditions unless specified otherwise. All ^{31}P NMR were proton decoupled. ^{31}P chemical shifts were measured relative to ~1% $P(OMe)_3$ in C_6D_6 sealed in coaxial capillaries but are reported in ppm from 85% H_3PO_4 ($\delta P(OMe)_3 = 140.4$ ppm). ^1H chemical shifts were measured relative to partially deuterated solvent peaks but are reported relative to tetramethylsilane. T_1 measurements were made by using the inversion recovery method.[1] Dynamic NMR spectra were simulated by using a modified version of the program DNMR4[60] and second-order spectra were simulated by using the LAOCN 5 program.[61]

Microanalyses were performed by the Canadian Microanalytical Service, Ltd. Fast atom bombardment mass spectrometry (FABMS) spectra were obtained with a VG 70-250S mass spectrometer by using a nitrophenyl octyl ether (NPOE) matrix. A PAR Model 273 potentiostat was used for cyclic voltammetry studies. The electrochemical cell contained a Pt working electrode, W secondary electrode, and Ag wire reference electrode in a Luggin–Haber capillary probe; THF or CH_2Cl_2 solutions were 0.002 M in the complexes and 0.2 M in n-Bu_4NBF_4. Reported potentials are referenced to ferrocene which was added to these solutions.

Preparation of *cis*- and *trans*-$OsH_2(dppe)_2$. Method 1. A slurry of $LiAlH_4$ (0.040 g, 1.05 mmol) in 5 mL of THF was added to a stirred suspension of 0.270 g (0.255 mmol) of *cis*-$OsCl_2(dppe)_2$ in 30 mL of THF. The mixture was refluxed for 15 min and cooled, and 7 mL of EtOH was added. After solvent evaporation, 20 mL of THF was added to the white residue, and the lithium salts were removed by filtration through THF saturated Celite, which was then rinsed with THF (2 × 10 mL). The pale yellow filtrate volume was reduced to dryness; 0.030 g (0.51 mmol) of NaCl and 20 mL of acetone was added, and the mixture was refluxed for 1 h to displace aluminium-containing ligands. The acetone was removed under vacuum, and the THF soluble portion of the residue, containing *cis*- and *trans*-$OsH_2(dppe)_2$ and *trans*-$OsHCl(dppe)_2$ in the approximate proportions of 7:1:3, respectively, was isolated by filtration through Celite. The pale yellow filtrate was concentrated to 20 mL, and $NaBH_4$ (0.017 g, 0.45 mmol) in 10 mL of EtOH was added. After stirring for 15 min the solvent was removed under vacuum, and the residue treated with THF and filtered through Celite. Concentration of the filtrate to 2 mL and addition of hexane (8 mL) caused precipitation of the pale lemon yellow product (0.238 g, 79%) which is a mixture of the cis and trans isomers: FABMS calcd for $C_{52}H_{50}{}^{192}OsP_4$ 990.2, observed 989 ($M^+ - H$) and 987 ($M^+ - 3\ H$); IR (Nujol) $\nu(OsH)$ 1964 cm^{-1} (m, br); *trans*-$OsH_2(dppe)_2$ $\delta(^1H, C_6D_6)$ −10.86 (quint, $J_{HP} = 15.5$ Hz), δ (^{31}P, THF) 49.6 (s); *cis*-$OsH_2(dppe)_2$ $\delta(^1H, C_6D_6)$ −9.95 (m), δ (^{31}P, 81 MHz, THF; A_2MN pattern, $J_{AM} \sim 5$ Hz, $J_{AN} \sim 5$ Hz, $J_{MN} < 5$ Hz) 45.7 (P_A, t), 35.9 (P_M, t), 35.6 (P_N, t). At higher field (162 MHz) an A_2M_2 pattern is observed in the ^{31}P NMR spectrum: $\delta_A = 45.7$, $\delta_M = 35.8$ ppm, $J_{AM} = 5.8$ Hz.

Method 2. *cis*-$OsCl_2(dppe)_2$ (0.138 g, 0.130 mmol) was dissolved in 25 mL of CH_2Cl_2. A slurry consisting of 0.034 g (0.35 mmol) of NaO^tBu, 0.55 g (0.16 mmol) of $NaBPh_4$, and 50 mL of a 20% ^tBuOH/80% THF solvent mixture was added to the yellow CH_2Cl_2 solution. The reaction mixture immediately turned orange upon addition of the salts. This color faded to pale yellow after ~2 min reaction with H_2. The slurry was left to stir under H_2 for 13 h. Then the reaction solution was pale yellow and contained a fine white precipitate. After evaporation of the solvents the bulk of the salts (NaCl, unreacted NaO^tBu and $NaBPh_4$) were removed by filtration through THF-saturated Celite as a THF (25 mL) solution. After evaporation of the straw yellow filtrate to dryness, 25 mL of benzene was added, and the insoluble material was removed by filtration through benzene-saturated Celite. The volume of the pale yellow filtrate was reduced to dryness. Precipitation from a THF solution (2 mL) by addition of hexanes (15 mL) gave the product as a white powder (0.130 g, 80%). ^1H NMR indicated 90% cis isomer and 10% trans isomer. Recrystallization can be effected by addition of a minimal volume of benzene to a boiling acetone slurry and then allowing the solution to cool. Anal. Calcd for $C_{52}H_{50}OsP_4$: C, 63.15; H, 5.09. Found: C, 63.49; H, 5.43.

Preparation of *cis*- and *trans*-$OsH_2(dppe\text{-}d_{20})_2$. Method 2 was employed except that the deuterated ligand was used and no CH_2Cl_2 was employed.

Preparation of *trans*-$[OsH(dppe)_2(\eta^2\text{-}H_2)]BF_4$, 1Os. $OsH_2(dppe)_2$ (0.245 g, 0.248 mmol) was suspended in 7 mL of diethyl ether. Under 1 atm of Ar 0.3 mL of $HBF_4\cdot Et_2O$ (excess) was added dropwise with stirring. The pale green suspension was stirred under H_2 atmosphere for 10 min, filtered under Ar atmosphere, and washed with diethyl ether (3 × 5 mL), which removed most of the green coloration: 0.225 g (84%) of the product was obtained. FABMS calculated for $C_{52}H_{51}{}^{192}OsP_4$ 991.2, observed 989 ($M^+ - 2\ H$) and 987 ($M^+ - 4\ H$), as with $OsH_2(dppe)_2$; $\delta(^1H, CD_2Cl_2$, 293 K) −7.35 (s, 3 H, $w_{1/2} = 115$ Hz), δ (^1H, CD_2Cl_2, 214 K, 200 MHz), 7.5–7.0 (m, 40 H, Ph), 2.1 (m, 8 H, CH_2), −6.80 (s, 2 H, H_2), −9.00 (quint, 1 H, $J_{HP} = -17$ Hz, OsH), $\delta(^{31}P$, acetone) 37.2 (s). Anal. Calcd for $C_{52}H_{51}BF_4OsP_4$: C, 58.00; H, 4.77. Found: C, 57.72; H, 4.87.

Preparation of *trans*-$[OsH(dppe\text{-}d_{20})_2(\eta^2\text{-}H_2)]BF_4$, 1Os. Excess $HBF_4\cdot Et_2O$ was added with stirring to a filtered, saturated solution of $OsH_2(dppe\text{-}d_{20})_2$ (60 mg) in 3 mL of THF. After 15 min the white precipitate was filtered, washed with 2 × 0.5 mL THF, and dried in vacuo [$\delta(^1H, CD_2Cl_2$, 200 MHz, 224.4 K) 2.09 (m, 8 H, CH_2), −6.83 (br s, 2 H, $\eta^2\text{-}H_2$), −8.98 (quint, $J_{HP} = -16.8$ Hz, 1 H, OsH)]. The inversion recovery T_1 determinations (Table III) were done at 225 and 195 K. The 180° pulse width was calibrated at each temperature by using the CH_2CH_2 resonance.

Preparation of $ReH_3(dppe)_2$, 3Re. $ReH_3(dppe)_2$ was first prepared by M. Freni et al. by the substitution reaction of dppe with $ReH_5(PPh_3)_3$ in the absence of solvents.[62] A modified preparation was used in this work. A mixture of 0.50 g (0.63 mmol) of $ReH_5(PMePh_2)_3$[63] and 0.55 g (1.38 mmol) of dppe in a Schlenk flask was heated at 180–200 °C under vacuum for 2 h. The reaction flask was cooled down to room temperature, and 2 mL of EtOH was added. The resulting mixture was stirred overnight to give a yellow solid. The solid was collected by filtration, washed with EtOH and acetone, and dried under vacuum overnight: yield 0.62 g, 59%.

Preparation of $[Os(H\cdots H)_2H(depe)_2]BPh_4$, 2Os. *trans*-$OsClH(depe)_2$ (0.10 g, 0.16 mmol) was dissolved in acetone (10 mL), and $NaBPh_4$ (57 mg, 0.17 mmol) was added under Ar. The mixture was stirred under H_2 for 30 min and then filtered through Celite. Concentration of the filtrate, and the addition of methanol caused precipitation of the white product (0.11 g, 72% yield): $\delta(^1H$, acetone-d_6, 200 K, 400 MHz) 7.3 (m, 8 H, BPh_4), 6.93 (m, 8 H, BPh_4), 6.78 (m, 4 H, BPh_4), 1.96 (br m, 8 H, PCH_2CH_2P), 1.63 (br d, $J_{HP} = 6.8$ Hz, 16 H, PCH_2), 1.00 (br d, $J_{HP} = 4.9$ Hz, 24 H, CH_3), −9.68 (quint, $J_{PH} = -17.5$, OsH), −10.03 (br s, OsH_2). Anal. Calcd for $C_{44}H_{71}BOsP_4$: C, 57.14; H, 7.74. Found: C, 56.80; H, 7.70.

The complex $[Os(H\cdots H)(H)(depe)_2]BF_4$ (see Table I) was prepared in an analogous fashion by using $NaBF_4$ instead of $NaBPh_4$ and a reaction temperature of 50°.

Preparation of 1Os-d_1. $OsH_2(dppe)_2$ (0.066 g, 0.067 mmol) was added to 10 mL of Et_2O containing 0.1 mL of D_2O. Approximately 0.05 mL of $HBF_4\cdot Et_2O$ was then added to produce DBF_4 in situ. The white precipitate was filtered and washed with three 5-mL volumes of Et_2O: ^1H NMR, Figure 4.

Preparation of Isotopomers 2Os-d_1. The gas HD was generated by adding NaH to D_2O. The complex **2Os**-d_1 was synthesized from HD, $NaBPh_4$, and *trans*-$OsClH(depe)_2$ as described above for **2Os**. MeOH was added to precipitate the product. This resulted in the formation of some **2Os**-d_0: ^1H NMR, Figure 6.

Preparation of Isotopomers 2Os-d_2. This complex was synthesized from D_2, $NaBPh_4$, and *trans*-$OsClH(depe)_2$ as described above for **2Os** except that acetone-d_6 was the solvent, and MeOD was the precipitating

---

(58) Chatt, J.; Hayter, R. G. *J. Chem. Soc.* **1961**, 896–904.

(59) Chatt, J.; Hayter, R. G. *J. Chem. Soc.* **1961**, 2605–2611.

(60) Bushweller, C. H.; Letenare, L. J.; Brunelle, J. A.; Bilofsky, H. S.; Whalon, M. R.; Fleischman, S. H. *Quantum Chemistry Program Exchange* No. 466, DNMR-4.

(61) Cassidei, L.; Sciacovelli, O. *Quantum Chemistry Program Exchange* No. 458, LAOCN 5.

(62) Freni, M.; Demichelis, R.; Giusto, D. *J. Inorg. Nucl. Chem.* **1967**, 1433–1439.

(63) Emge, T. J.; Koetzle, T. F.; Bruno, J. W.; Caulton, K. G. *Inorg. Chem.* **1984**, *23*, 4012.

(64) Moehring, G. A.; Walton, R. A. *J. Chem. Soc., Dalton Trans.* **1987**, 715–720.

(65) Kubas, G. J.; Ryan, R. R.; Wrobleski, D. A. *J. Am. Chem. Soc.* **1986**, *108*, 1339–1341.

agent: **Os**-d_2, was obtained in 50% yield; ^{1}H NMR, Figure 5.

Preparation of 3Re-d_2. One milliliter of D_2O was added to a 3 mL of acetone-d_6 containing 50 mg (0.049 mmol) of $[ReDH_3(dppe)_2]Cl$[62] prepared by protonation of $ReH_3(dppe)_2$ with aqueous DCl solution in benzene. The ^{1}H NMR spectrum of this mixture after 1 week indicated a composition close to $[ReD_{2.7}H_{1.3}(dppe)_2]Cl$. The solution was evaporated to dryness in vacuo. The residue was redissolved in 3 mL of THF and then reacted with 2 mL of 1.6 M *n*-BuLi in hexane. After the reaction mixture was stirred for 10 min, 2 mL of EtOH were added to neutralize the excess BuLi. The solvent was removed under vacuum, and the residue was extracted with benzene. The benzene was removed under vacuum, and the yellow residue was washed with 2 mL of EtOH to give a yellow powder. The powder was collected by filtration, washed with EtOH, and dried in vacuo overnight: yield 34 mg, 68%. Integration of resonances in the ^{1}H NMR spectrum gave the composition $ReD_{2.2}H_{0.8}(dppe)_2$.

Preparation of *trans*-[Os(CO)H(dppe)$_2$]BF$_4$. **1Os** was prepared in situ from 0.085 g (0.086 mmol) of $OsH_2(dppe)_2$ and $HBF_4{\cdot}Et_2O$. The reactant was dissolved in 15 mL of acetone yielding a clear solution. The solution was degassed with CO and allowed to stir under CO for 31.5 h. A ^{31}P NMR spectrum indicated that H_2 displacement was complete. After obtaining ^{1}H NMR and IR spectra the remaining product was crystallized from acetone by slow Et_2O diffusion: IR (CH_2Cl_2) ν(CO) 2002.5 s, ν(OsH) 1916.5 cm^{-1} w; δ(^{1}H, acetone-d_6) −7.87 (quint, J_{HP} = 19.2 Hz, 1 H), δ(^{31}P, acetone) 30.4 (s). Anal. Calcd for $C_{53}H_{49}BF_4OOsP_4$: C, 57.77; H, 4.47. Found: C, 57.37; H, 4.52.

Reaction of 2Os with Carbon Monoxide. The complex (0.091 g, 0.098 mmol) in 10 mL of acetone at 20° was reacted with CO (1 atm). The rate of loss of **2Os** was monitored by ^{31}P NMR and shown to be first order in [**2Os**] with $t_{1/2}$ = 170 h. *trans*-$[OsH(depe)_2(CO)]^+$[34] was the only product: δ(^{31}P, acetone) 27.7 (s).

Note Added in Proof. Brammer et al.[66] have reported an "intermediate" H–H distance of 1.357 (7) Å in the complex $ReH_7(Ptol_3)_2$. This was a single-crystal neutron diffraction study. Thus structure **2**, Figure 1, is feasible for complex **2Os**. It is not yet known whether this Re complex will have T_1 and J(H,D) coupling behavior similar to that of **2Os**-d_2.

Acknowledgment. This work was supported by grants to R. H. M. from NSERC Canada and the donors of the Petroleum Research Fund, administered by the American Chemical Society, and a loan of Ru and Os chlorides from Johnson Matthey Ltd. We thank Dr. Leslie Field, Dr. Robert Crabtree, and Dr. Doug Stephan for useful discussions, E. P. Cappellanni and Nick Plavac for VT T_1 measurements, and T. E. Burrow for computer programming.

---

(66) Brammer, L.; Howard, J. A. K.; Johnson, O.; Koetzle, T. F.; Spencer, J. L.; Stringer, A. M. *J. Chem. Soc., Chem. Commun.*, in press.

Multifield Saturation Magnetization and Multifrequency EPR Measurements of Deoxyhemerythrin Azide. A Unified Picture

Michael P. Hendrich,[†] **Linda L. Pearce,**[‡] **Lawrence Que, Jr.,**[‡] **N. Dennis Chasteen,**[§] **and Edmund P. Day**[*,†]

Contribution from the Gray Freshwater Biological Institute, University of Minnesota, Navarre, Minnesota 55392, the Department of Chemistry, University of Minnesota, Minneapolis, Minnesota 55455, and the Chemistry Department, University of New Hampshire, Durham, New Hampshire 03824. *Received September 27, 1990*

Abstract: The magnetic properties of deoxyhemerythrin azide have been measured by combining multifield saturation magnetization data and multifrequency EPR spectra. The exchange coupling [J = −3.4 (1) cm^{-1}; $J\mathbf{S}_1{\cdot}\mathbf{S}_2$], average zero-field splitting parameters [$|D_1| = |D_2|$ = 12 (1) cm^{-1} and $E_1/D_1 = E_2/D_2$ = 0.3], and average g values [$g_1 = g_2$ = 2.23 (5)] have been determined assuming identical iron sites with parallel zero-field splitting axes for the ferromagnetically coupled high-spin diferrous center. The observed ratio of the exchange coupling to the zero-field splitting (J/D_i = 0.28) lies in the weak exchange coupling regime of a perturbation treatment of the full 25 × 25 spin Hamiltonian of the coupled diiron center. Perturbation expressions required for the description of the integer-spin EPR signals of two S = 2 metals in either the strong ($J/D_i > 1$) or weak ($J/D_i < 1/3$) exchange coupling regimes are presented. For deoxyhemerythrin azide the EPR signal arises from the lowest pair of energy levels of the coupled system and can be interpreted in either coupling regime. The saturation magnetization family of curves, on the other hand, are a thermal average of all levels populated from 2 to 200 K and can resolve this ambiguity in the interpretation of the EPR data. An excellent fit to the entire family of multifield saturation magnetization curves has determined both the exchange coupling and zero-field splitting of deoxyhemerythrin azide, which lies in the weak coupling regime. In addition, quantitative agreement between saturation magnetization, integer-spin EPR, and optical data has been obtained.

Hemerythrin is a well-characterized oxygen-storage protein isolated from several marine organisms.[1,2] For deoxyhemerythrin the active site consists of two high-spin iron atoms that are bridged by a hydroxo group[3,4] and two carboxolato groups, one each from an aspartate and a glutamate residue.[5] Five of the remaining coordination sites of the diiron center are histidine residues, leaving a single coordination site available for exogenous ligands. In deoxyhemerythrin the two high-spin ferrous ions are antiferromagnetically coupled with J estimated to be between 20 and 70 cm^{-1} ($J\mathbf{S}_1{\cdot}\mathbf{S}_2$).[1,2,4,6,7] Reem and Solomon showed, in studies combining magnetic circular dichroism (MCD) and EPR, that upon addition of azide to deoxyhemerythrin the exchange coupling

---

[*] Address correspondence to this author at the Department of Physics, Emory University, Atlanta, GA 30322.

[†] Gray Freshwater Biological Institute, University of Minnesota.

[‡] Department of Chemistry, University of Minnesota.

[§] Chemistry Department, University of New Hampshire.

(1) Klotz, I. M.; Kurtz, D. M., Jr. *Acc. Chem. Res.* **1984**, *17*, 16–22.

(2) Wilkins, P. C.; Wilkins, R. G. *Coord. Chem. Rev.* **1987**, *79*, 195–214.

(3) Reem, R. C.; Solomon, E. I. *J. Am. Chem. Soc.* **1984**, *106*, 8323–8325.

(4) Zhang, K.; Stern, E. A.; Ellis, T.; Sanders-Loehr, J.; Shiemke, A. K. *Biochemistry* **1988**, *27*, 7470–7479.

(5) Stenkamp, R. E.; Sieker, L. C.; Jensen, L. H.; McCullum, J. D.; Sanders-Loehr, J. *Proc. Natl. Acad. Sci. U.S.A.* **1985**, *82*, 713–716.

(6) Maroney, M. J.; Kurtz, D. M.; Nocek, J. M.; Pearce, L. L.; Que, L. *J. Am. Chem. Soc.* **1986**, *108*, 6871–6879.

(7) Reem, R. C.; Solomon, E. I. *J. Am. Chem. Soc.* **1987**, *109*, 1216–1226.

0002-7863/91/1513-3039$02.50/0 © 1991 American Chemical Society